Ryerson University
Digital Commons @ Ryerson

Theses and dissertations

1-1-2012

AC-DC Microgrid Optimal Power Flow

Inderjeet Duggal
Ryerson University

Follow this and additional works at: http://digitalcommons.ryerson.ca/dissertations

Part of the Digital Circuits Commons, and the Power and Energy Commons

Recommended Citation
Duggal, Inderjeet, "AC-DC Microgrid Optimal Power Flow" (2012). *Theses and dissertations.* Paper 975.

This Thesis is brought to you for free and open access by Digital Commons @ Ryerson. It has been accepted for inclusion in Theses and dissertations by an authorized administrator of Digital Commons @ Ryerson. For more information, please contact bcameron@ryerson.ca.

AC-DC MICROGRID OPTIMAL POWER FLOW

by

Inderjeet Duggal

B.Eng, Ryerson University, 2010

A thesis

presented to Ryerson University

in partial fulfillment of the

requirements for the degree of

Master of Applied Science

in the Program of

Electrical and Computer Engineering

Toronto, Ontario, Canada, 2012

© Inderjeet Duggal 2012

AUTHOR'S DECLARATION FOR ELECTRONIC SUBMISSION OF A THESIS

I hereby declare that I am the sole author of this thesis. This is a true copy of the thesis, including any required final revisions, as accepted by my examiners.

I authorize Ryerson University to lend this thesis to other institutions or individuals for the purpose of scholarly research.

I further authorize Ryerson University to reproduce this thesis by photocopying or by other means, in total or in part, at the request of other institutions or individuals for the purpose of scholarly research.

I understand that my thesis may be made electronically available to the public.

AC-DC MICROGRID OPTIMAL POWER FLOW

Master of Applied Science, 2012

Inderjeet Duggal

Electrical and Computer Engineering

Ryerson University

ABSTRACT

Electricity market deregulation has opened the door for novel electricity production schemes within the existing central production paradigm that dominates the electricity power industry. The Microgrid concept allows generation and load located in close vicinity to be organized so that the local load is served as far as possible with local generation. The Microgrid examined in this thesis consists of both AC and DC network components connected using power converters.

The varied Microgrid power sources (microturbine generators, PV, battery, power imports from the grid etc.) are scheduled over 24 hours to satisfy load demand at minimum cost and maximum reliability. Towards this end, a dual objective problem is formulated using Fuzzy sets and the final problem takes the form of a Mixed-Integer Nonlinear optimization problem. The interplay between the disparate objectives of minimum cost and maximum reliability and the battery is then examined.

ACKNOWLEDGEMENTS

Many thanks to my supervisor, Professor Bala Venkatesh, for all his support and guidance throughout the research work. All the support from my family and friends is also greatly appreciated. Also, thanks to everyone in the lab and the ELCE Department for always offering their assistance.

TABLE OF CONTENTS

CHAPTER 1: INTRODUCTION **1**

CHAPTER 2: MICROGRIDS **4**

2.1 MICROGRIDS AND SYSTEM COMPONENTS 4

2.1.1 Generation *4*

2.1.2 Storage *5*

2.2 DC MICROGRIDS 5

CHAPTER 3: AC-DC LOAD FLOW AND CONVERTER THEORY **8**

3.1 AC-DC LOAD FLOW BASICS 8

3.2 CONVERTER THEORY 10

3.2.1 Converter Circuit *11*

3.2. 2 Rectification, Inversion and Commutation *13*

3.2.3 AC line current under commutation *16*

3.2.4 DC voltage under commutation *16*

3.2.5 Inverter Voltage Equation *17*

3.2.6 AC Current Fundamental Component (RMS) *19*

3.2.7 AC Power Factor - Rectifier *19*

3.3 CONVERTER MODEL 20

3.3.1 DC per unit system *20*

3.3.2 Control Equations *23*

3.3.3 Converter Power in terms of the DC System Variables *23*

3.3.4 Summary *24*

CHAPTER 4: AC-DC OPF PROBLEM FORMULATION **26**

4.1 PROBLEM FORMULATION 26

4.1.1 Economic Objective *26*

4.1.2 Dual Objectives - Economic and Reliability Objectives *27*

4.2 AC NETWORK EQUATIONS 29

4.2.1 AC Generator Equations *29*
4.2.2 Load Bus Equations *30*
4.2.3 Power Import Bus Equations *30*
4.2.4 Converter Bus Equations *30*
4.3 CONVERTER EQUATIONS 31
4.4 DC NETWORK EQUATIONS 32
4.4.1 DC Load Buses *32*
4.4.2 DC Buses that have a Battery *33*
4.4.3 DC Converter buses *33*
4.4.3 DC Buses that have a PV Array *33*
4.4.4 Battery Equations *34*
CHAPTER 5: TEST CASE AND RESULTS 37
5.1 TEST CASE MICROGRID 37
5.1.1 AC Network Components *37*
5.1.2 DC Network Components *38*
5.2 TEST-CASE (MICROGRID WITH 14 BUS AC SYSTEM AND 7 BUS DC SYSTEM) 40
5.2.1 AC System *40*
5.2.2 DC System *41*
5.2.3 System Load Data, PV Forecast and Market Price *42*
5.3 RESULTS (NO RESERVE) 43
5.4 RESERVE 47
5.4.1 Results (4 hr Reserve) *47*
5.5 ENERGY IN THE BATTERY FOR DIFFERENT RESERVE REQUIREMENTS 50
5.6 DUAL OBJECTIVE – MINIMIZE COST AND MAXIMIZE RELIABILITY 51
CHAPTER 6: CONCLUSIONS 55
APPENDICES 58
APPENDIX A: ALTERED IEEE 14-BUS SYSTEM, FIG. 10 58
APPENDIX B: DC NETWORK, FIG. 11 65
APPENDIX C: CONVERTERS 67
APPENDIX D: NETWORK SOLUTION 68

REFERENCES.....78

LIST OF TABLES

TABLE 1: GENERATOR COST FUNCTIONS 40
TABLE 2: CONVERTER CONTROLS 41
TABLE 3: CONVERTER UNKNOWNS 46

LIST OF FIGURES

FIGURE 1 AC-DC MICROGRID MODEL 7
FIGURE 2 CONVERTER CONNECTING AC AND DC NETWORKS 9
FIGURE 3 TRANSFORMER AND 6-PULSE CONVERTER, [11] 11
FIGURE 4 12-PULSE CONVERTER 12
FIGURE 5 6-PULSE CONVERTER CIRCUIT, [11] 13
FIGURE 6 CONVERTER WAVEFORMS FOR RECTIFICATION, [11] 14
FIGURE 7 CONVERTER WAVEFORMS FOR INVERSION, [11] 14
FIGURE 8 CURRENT COMMUTATION, [11] 15
FIGURE 9 AC BUS, TRANSFORMER AND CONVERTER 21
FIGURE 10 IEEE 14 BUS SLIGHTLY ALTERED 38
FIGURE 11 MICROGRID DC SYSTEM 39
FIGURE 12 TOTAL REAL POWER DEMAND 42
FIGURE 13 PV ARRAYS PRODUCTION FORECAST 42
FIGURE 14 MARKET PRICE 43
FIGURE 15 GENERATOR SCHEDULE 44
FIGURE 16 POWER IMPORT FROM GRID AND BATTERY SCHEDULE 45
FIGURE 17 PV ARRAY POWER PRODUCTION AND BATTERY SCHEDULE 45
FIGURE 18 GENERATOR SCHEDULE 48
FIGURE 19 POWER IMPORT FROM GRID AND BATTERY SCHEDULE 49
FIGURE 20 TOTAL COST AND POWER LOSS 50
FIGURE 21 ENERGY IN BATTERY FOR RESERVE REQUIREMENTS RANGING FROM 0 TO 4 HRS 50
FIGURE 22 POWER IMPORT AND BATTERY SCHEDULE 52
FIGURE 23 ENERGY STORED IN BATTERY 53
FIGURE 24 COST AND RELIABILITY VS. BATTERY CAPACITY (KWH) 53
FIGURE 25 COST AND RELIABILITY VS. BATTERY CAPACITY (KWH) 54

LIST OF SYMBOLS

P_c^{sch}, Q_c^{sch}	Scheduled power injection at the converter terminal bus
$P_c(AC), Q_c(AC)$	Real and reactive power injected by AC network at the converter terminal AC bus
$P_c(DC), Q_c(DC)$	Real and reactive power injected by converter at the converter terminal AC bus
V_c	AC voltage at the converter terminal bus
$\bar{x}$	DC system variables
$R(V_c, \bar{x})$	Converter equations
V	AC bus voltage
θ	AC bus angle
P_{DC}	DC network power injection
V_{dc}	DC network nodal voltage
L_c	AC line inductance
L_d	DC line inductance
a	Transformer tap
X_c	Commutation reactance (taken to be 0.05)
α	Converter firing delay angle
μ	Commutation angle
γ	Extinction advance angle
ω	AC line frequency
I_d	DC current
V_d	DC voltage
V_{co}	$= \frac{3\sqrt{2}}{\pi} aV_c$
k_1	$k\frac{3\sqrt{2}}{\pi}$, where k=1 under normal operation
I_1	AC line current fundamental (RMS)
ϕ	Phase difference between AC fundamental voltage and current
k, n	Bus index

c	AC buses connected to power converters
t	Time index
NG	Number of AC generator
NT	Number of hours (24)
NB	Number of AC buses
NDC	Number of DC buses
Y_{kn}	AC network admittance magnitude between buses k and n
θ_{kn}	AC network impedance angle between buses k and n
$V_{d,c,t}$	Converter DC voltage at the kth converter bus at time t
$V_{dc,c,t}$	DC voltage at the kth bus of the DC network at time t
$V_{n,t}$ (or $V_{k,t}$)	AC voltage at bus n (or bus k) at time t
$P_{k,t}$	Power injected into the AC network at k^{th} bus at time t
$P_{c,t}$(AC), $P_{c,t}$(DC)	Real power injected into the converter terminal bus c by the AC system and the real power flowing through the converter at time t
$Q_{c,t}$(AC), $Q_{c,t}$(DC)	Reactive power injected into the network at the converter terminal bus c by the AC and DC networks at time t
$PG_{k,t}$	AC power generation at the kth AC bus
$PD_{k,t}$	AC power demand at the kth AC bus
$P_{import,t}$	Power import from the grid
MP_t	Market Price at time t
BPC_t , BPD_t	Battery charging and discharging at time t
$P_{dc,1,t}^{sch}$, $P_{dc,5,t}^{sch}$	Scheduled DC load at DC buses 1 and 5 at time t
$PV_{6,t}^{sch}$, $PV_{6,t}^{sch}$	PV production at DC buses 6 and 7 at time t
$BPDUPPER_t$	Battery charging power upper limit
$BPCUPPER_t$	Battery charging power lower limit
UPD_t	Binary variable indicating if battery discharges (1) or not (0) at time t
UPC_t	Binary variable indicating if battery charges (1) or not (0) at time t
$RESERVE_t$	Reserve required in battery at time t
$BATTERYCAPACITY_t$	
CC	Battery charge cycle cost

S_t	Binary variable indicating charge cycle start (1 = charge cycle start, 0 = otherwise) at time t
COST(PG, P_{import}, S)	Total cost of satisfying load
$Cost_{max}$ and $Cost_{min}$	Maximum cost and minimum cost used in the Fuzzy formulation
TEB_t	Total energy stored in the battery at time t
TEB_{max} and TEB_{min}	Total Energy in the Battery maximum and minimum
μc	Fuzzy satisfaction function for cost
μe_t	Fuzzy satisfaction function for Total Energy in the Battery
λ	Minimum of all the fuzzy satisfaction functions

ABBREVIATIONS AND ACRONYMS

MP	Market Price
OPF	Optimal Power Flow
MINLP	Mixed Integer Non-Linear Programming
MGCC	Microgrid Central Controller
RI	Reliability Index

CHAPTER 1: INTRODUCTION

Microgrids are small localized power systems where the power demands of the local load is met as much as possible with local generation which tends to be much more varied than in large power systems. The local organization and central control of the Microgrid allows for a much more varied generation portfolio which would not necessarily be economical in a large centralized power system. With varied generation, which can range from microturbine generators, fuel cells, PV arrays, wind turbines, batteries and other power sources, the scheduling of Microgrids becomes an important problem complicated by the presence of the myriad of system components which includes power converters.

Microgrids as an alternative to small scale LV AC distribution systems require some justification. The operation of a Micorgrid opens up some economic possibilities for both the producers and the consumers which would not be present otherwise. The Microgrid sources may be able to sell at prices above the norm and the consumers may be able to get prices below retail prices. If the Microgrid is allowed to trade power over the grid with the overlying network and depending on the price structure present, the Microgrid will be in a favourable situation both from an economic point of view and reliability point of view. The Microgrid could assist the main network with ancillary services such as voltage and frequency control or relieve peak loading of network devices to offer technical benefits. Further, a self-sufficient Microgrid could decrease main network line flows. The physical closeness of the sources and loads also presents social benefits where both the consumers and producers are more aware of each other`s needs; for example, the producers have access to better forecasting due to the small size of the Microgrid and consumers are more aware about issues such as greenhouse gases and can dictate the Microgrid mandate within reason.

The scheduling of Microgrids has been explored in a variety of directions. Unit commitment in Microgrids by the improved genetic algorithm is discussed in [1]. The Microgrid contains distributed generators, storage devices and controllable loads all under the control of a management system. This work uses a simulated annealing technique to improve the convergence of the genetic algorithm which is used to schedule the Microgrid. The result presented in the paper schedules the Microgrid over 24 hours so that generation, battery status

and power imports and exports are determined. The main functions of the Microgrid central controller (MGCC) are highlighted in [2]. The centralized control of a Microgrid which operates in grid interconnected mode is given in [3]. Demand side bidding options for controllable loads are also incorporated into the formulation. The MGCC is identified as responsible for economic scheduling, short term load forecasting, security assessment and demand side management functions. Microgrids with both power and heat demands have also been investigated as in [4] where a dynamic programming solution for an AC-DC Microgrid with both an electricity and heat demands with the goal of maximizing the profit is given. Cost optimization and fuel consumption minimization are explored in [5]. The optimization seeks to meet the local energy demand while minimizing the fuel consumption. Penalties are also applied to any excess heat produced to stay consistent with the environmentally friendly operation as indicated by the renewable penetration. A hybrid of the genetic algorithm and Lagrangian relaxation is used to find a least operating cost schedule of the Microgrid in [6]. Microgrids also find applciations in ancilliary services and the case of several Microgrids providing frequency control reserves when the Microgrids operate under decentralized or centralized control is investigated in [7].

Whereas the majority of the papers highlighted above consider the scheduling of AC Microgrids, the case of an AC-DC Microgrid is examined in this thesis. A Microgrid consisting of both an AC and a DC network allows AC network elements such as AC generation and loads and DC network elements such as batteries, fuel cells, PV arrays, DC loads etc. to be separated. The AC and DC components of the Microgrid are separated by power converters to exchange power thus the converters need to be modeled in the scheduling. The role of the battery is also heavily emphasized in this thesis not only for temporal shifting of energy but also for reliability purposes. The battery allows energy from energy imports from the grid and PV production to be stored and used at opportune times. The role of the battery as a reserve, to increase Microgrid reliability, for several hours is also considered.

Chapter 2 presents some background on Microgrids. Particular highlights include the types of power generation that are used in Microgrids, the types of storage which are viable at the Microgrid scale and the topology of a typical Microgrid. The topology considered in this thesis is also shown.

Chapter 3 covers AC-DC load flow and converter theory. The need to accommodate power converters and to handle both AC and DC networks in load flow requires that the load flow algorithm be altered slightly. This chapter starts out covering the basic theory of the 6-pulse converter and derives the equations necessary to model the converter in load flow.

Chapter 4 has the OPF formulation for the economic and reliable operation of the Microgrid. Two formulations are considered, the first formulation considers a minimum cost scheduling of the Microgrid and the second formulation considers a minimum cost and maximum reliability scheduling of the Microgrid where in both formulations the load is served using some combination of Microgrid AC generation, PV arrays, battery and power imported from the grid.

Chapter 5 presents the results for two cases. The first case is the scheduling of the Microgrid with the only objective being minimum cost and the second case considers the minimum cost and maximum reliability scheduling.

Chapter 6 offers conclusions based on the results and possible extensions of the problem for future work.

The network data and other information are shown in the Appendices.

CHAPTER 2: MICROGRIDS

2.1 Microgrids and System Components

Due to the small localized scale of the Microgrid, the power choices that would not be suitable for a large power system, due to technical or economic reasons or otherwise, turn out to be good choices for the Microgrid. For example, renewable energy penetration from PV arrays and wind turbines combined with a battery for suppressing intermittency proves to be much more viable at the power scale of a Microgrid. Storage devices also find more appropriate uses at the Microgrid scale than in a large power system. A detailed summary of the various generation and storage technologies can be found in [8]. The basics of these technologies are summarized below.

2.1.1 Generation

Microturbine generators are based on automotive turbo charger and military engine technologies. The high-speed rotation of the shaft produces high frequency AC power which is converted to DC and then back to 60 Hz AC power using a rectifier and inverter respectively. Microturbine generators commonly use natural gas as a fuel (diesel or jet fuel can also be used) and can approach efficiencies close to 70-80% using waste heat utilization (around 20-30 % without) with power ratings of several hundred kilowatts. Fuel cells convert chemical energy (using hydrogen as a fuel) to DC electrical energy and produce low emissions approaching efficiencies of around 40% while having ratings of several hundred kilowatts. Photovoltaic (PV) cells convert solar energy to electrical energy with the DC voltage produced depending on the number and type of cells. The efficiency values of PV devices range from 10-20%. PVs produce no emissions but they have high initial costs and their production is intermittent in nature. Wind generation also finds use at the Microgrid scale with wind generators at the power ratings of around 250 kW. If the Microgrid has both power and heat demands then combined heat and power (CHP) plants often find application where power and heat are produced more efficiently than if were to be produced separately.

2.1.2 Storage

Storage can play a much more important role at the Microgrid scale due the storage sizes being commensurate with many of the needs of the Microgrid. Due the nature of the energy sources in the Microgrid, storage devices can enhance the Microgrid reliability. Energy production and consumption do not have to occur at the same time; e.g. CHP plants can meet the heat demand and store the energy produced if it is not immediately needed. Also, storage is a good economic solution allowing power to be purchased and stored in off-peak hours from the grid. Lead acid batteries are available in almost any size and are commonly used. Flywheels store energy as kinetic energy in high speed rotating wheel or disk spinning at around 10, 000 rpm. Another option is superconducting magnetic energy storage which stores energy in a circulating current in a coil of superconducting wire.

2.2 DC Microgrids

AC power systems dominate when energy is required to be transferred over long distances due to voltage level conversion ease and the resultant reduction of transmission losses when power is transferred at high voltage levels. Since, in a typical Microgrid, the energy source is located very close to the load, small scale production becomes promising and worth considering in preference to large scale central AC power production. Newer technologies such as microturbine generation, CHP plants utilizing waste energy to increase efficiency, fuel cells producing electricity with very low emissions, batteries to store energy among others offer potentially viable alternatives to large scale central production although they still have a long way to go economically.

An AC power system with power converters installed faces a number of technical challenges that must be dealt with. Common problems caused by power converters include adverse impact on quality of supply, power losses along the lines due to harmonics and line overloads due to harmonic pollution. Passive and active filtering, UPS, “network friendly” converters and other solutions are used to mitigate these problems as discussed in [9]. The low electric fields associated with DC power lines also open up other avenues for DC systems such

as their use in underground cable systems and also their use in hospitals and other field sensitive areas such as military.

The Microgrid model in Figure 1 has an AC-DC Microgrid connected to the main grid to ensure high reliability; this model is similar to the model in [9] where only an AC Microgrid is considered. Separate AC and DC components in the Microgrid allow the Microgrid to take advantage of both AC and DC technologies. The converters can be centralized so that the harmonic pollution on the AC side is managed and proper constant voltage on the DC side is achieved. The Microgrid operation is under the control of the Microgrid Central Controller (MGCC) which is responsible for the operation of the Microgrid. The MGCC is responsible for the ensuring the operation of the Microgrid according to the mandate of the Microgrid which could be to provide ancillary services to the main grid, to operate as an island in an environmentally friendly manner, to operate in a low cost economic manner or other customized mandates. In order to achieve the Microgrid operational goal, the MGCC must not only direct local Microgrid operations but also negotiate with the system operator as to the Microgrid's role and responsibilities pertaining to the larger grid.

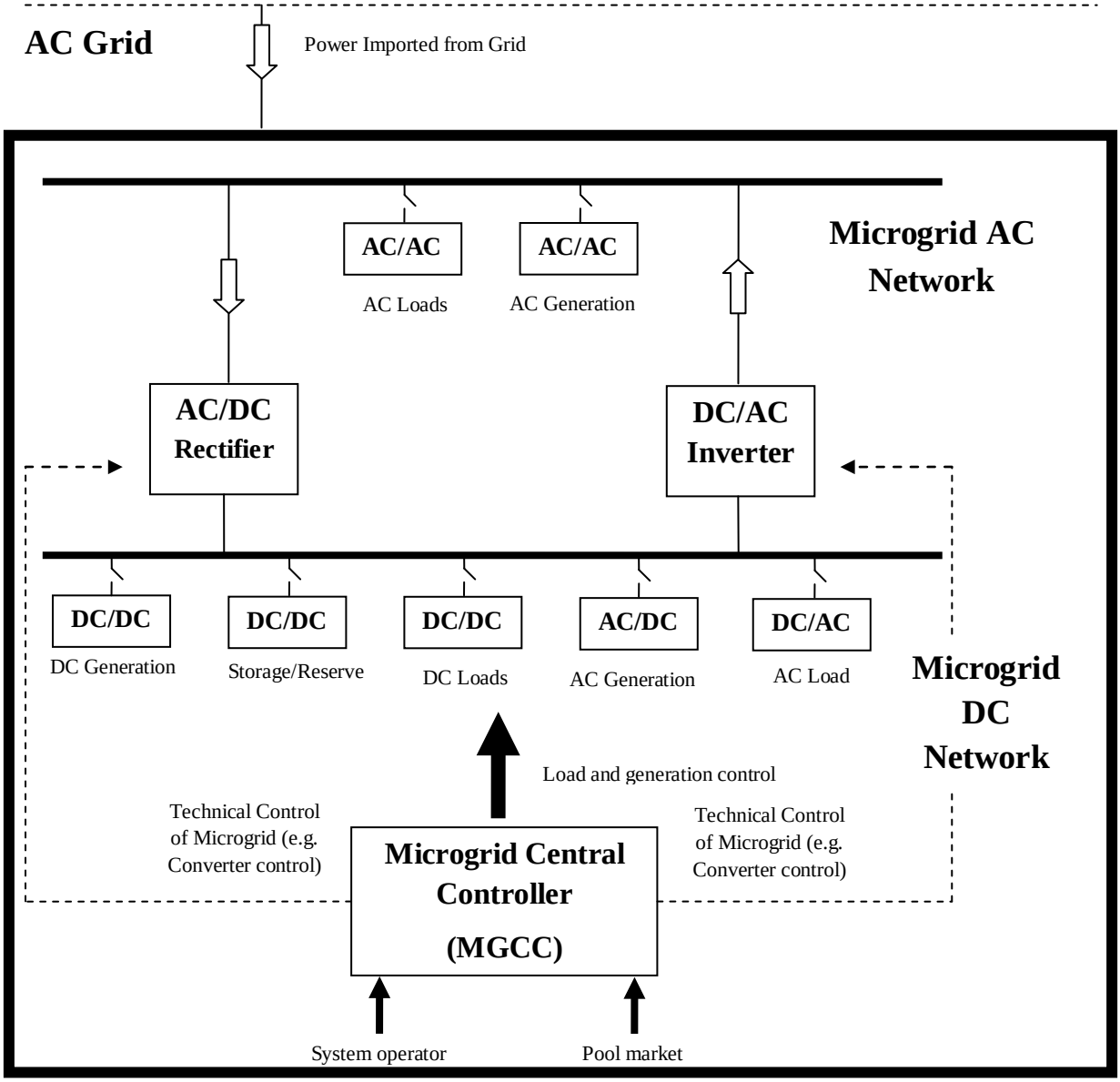

Figure 1 AC-DC Microgrid Model

Chapter 3: AC-DC Load Flow and Converter Theory

The AC system, the DC system and the power converters need to be represented in load flow and thus a converter model that can be used in load flow is required. The model presented in this chapter is based largely on [10], [11] and [12]. This model or variants of it can also be found in publications such as [13], [14], [15] and [16]. The thrust of this chapter is to describe steady state passive network equivalents of converters for use in AC-DC load flow and not researching on it. Firstly, the basics of AC-DC load flow will be described and then a model of the converter will be presented. The end result will be the derivation of the necessary equations to incorporate power converters into load flow.

3.1 AC-DC Load Flow Basics

AC load flow, [17], is a well understood and thoroughly researched topic but the incorporation of a DC network and power converters alters the problem slightly and AC load flow takes the form of AC-DC load flow. AC-DC load flow is required to incorporate power converters with typical applications found when DC links are modeled in power flow. In this work, the Microgrid has separate AC and DC power networks and thus converters are required to transfer power between these two networks. The power flow model of the AC-DC network takes the form of nonlinear equations which contains the traditional AC network power flow equations, the DC network power flow equations and the converter equations.

If the AC bus c has a converter attached to that bus, then the power flow equation at that bus, equations (3.1) and (3.2), needs to be altered to take account of the converter power flow.

$$P_c^{sch} - P_c(AC) - P_c(DC) = 0 \tag{3.1}$$

$$Q_c^{sch} - Q_c(AC) - Q_c(DC) = 0 \tag{3.2}$$

At each bus that has a converter, the AC power injection, the DC power injection and the load should balance. So, if a rectifier (transferring power from the AC to the DC system) and a load

are connected to a bus then the AC system will support the load and the rectifier which also is an effective load. P_c(AC) and Q_c(AC) are the real and reactive powers injected into the converter AC bus terminal in terms of the AC system variables and P_c(DC) and Q_C(DC) are the real and reactive powers injected into the converter AC bus terminal in terms of the AC and DC variables.. As will be seen in the theory section, the converter model used absorbs reactive power whether operating as a rectifier or an inverter. The power balance at the converter AC bus is shown in Figure 2.

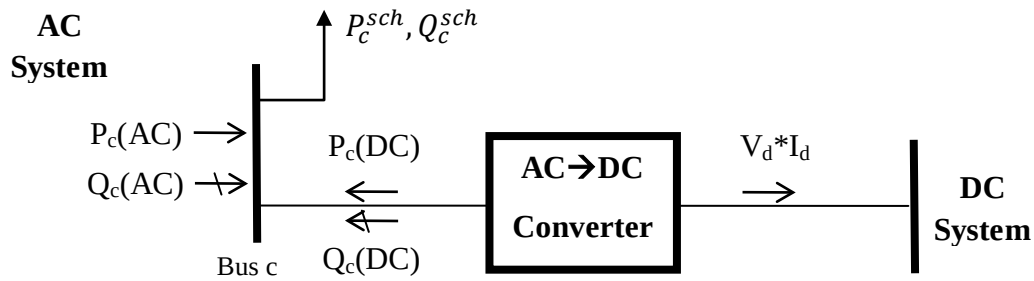

(a) Converter operating as a rectifier

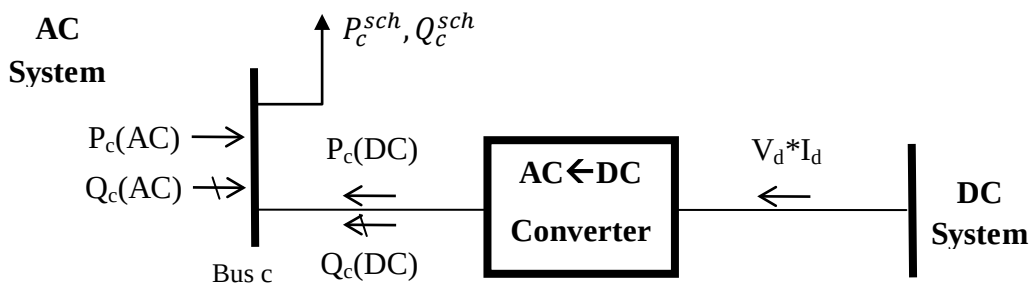

(b) Converter operating as an inverter

Figure 2 Converter connecting AC and DC networks

Both $P_c(DC)$ and $Q_c(DC)$ are a function of the ac system terminal voltage, V_c, and DC system variables $\bar{x}$. The functional representational is stated symbolically in (3.3) and (3.4).

$$P_c(DC) = f(V_c, \bar{x}) \tag{3.3}$$

$$Q_c(DC) = f(V_c, \bar{x}) \tag{3.4}$$

Equations derived from converter analysis are represented by

$$R(V_c, \bar{x}) = 0 \tag{3.5}$$

For each unknown related to the DC system and converter, there needs to be 1 equation and thus the number of equations in (3.5) and the number of unknowns must be the same.

The AC-DC power flow problem may be stated as

$$\begin{bmatrix} P^{sch} - P(V,\theta) \\ P_c^{sch} - P_c(V,\theta,\bar{x}) \\ Q^{sch} - Q(V,\bar{\theta}) \\ Q_c^{sch} - Q_c(V,\theta,\bar{x}) \\ R(V_c,\bar{x}) \\ P_{DC}^{sch} - P_{DC}(V_{dc}) \end{bmatrix} = 0 \tag{3.6}$$

The AC power flow equations at the converter terminal c are listed separately in (3.6) since the power flow equations have to be altered according to (3.1) and (3.2). The converter relations $R(V_c, \bar{x}) = 0$ and the DC network nodal equations are added to the usual AC load flow equations and the whole system is solved together in (3.6). The solution obtained from (3.6) gives the voltages and angles at AC system buses, the converter unknown variable values and the DC system nodal voltages.

The choice of the converter and DC system variables in $\bar{x}$ can be can be explained by briefly reviewing converter theory. The equations required to incorporate converters into load flow will now be derived below.

3.2 Converter Theory

The converter theory is based on [10], [11], and [12] with the final form of the equations in (3.6) being the same as in [10]. However, some more detail is presented in the derivations as compared to these works to make the results a little more clear. The converter relations $R(V_c, \bar{x}) = 0$ in equation (3.6) will now be derived.

3.2.1 Converter Circuit

The 6-pulse converter, shown in Figure 3, is the basic component used to convert power from AC to DC and vice versa. The converter is connected to the AC system using a transformer with on-load taps on the AC side to control the converter voltage. In Figure 3, the AC side of the transformer is star connected with a grounded neutral. The secondary side of the transformer is delta connected or star connected with an ungrounded neutral.

The upcoming analysis is all based on the 6-pulse converter for simplicity. However, the usual converter setup used to interface DC and AC power is a 12-pulse converter, Figure 4, where two 6 pulse bridges are used. The two converter bridges are supplied with voltages displaced by 30 degrees which helps reduce the ripple in the DC voltage and thus results in lower harmonic pollution.

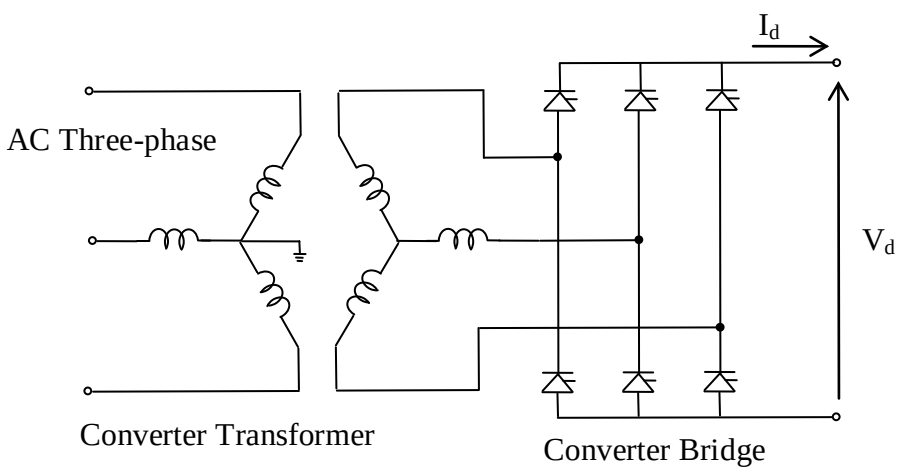

Figure 3 Transformer and 6-Pulse Converter, [11]

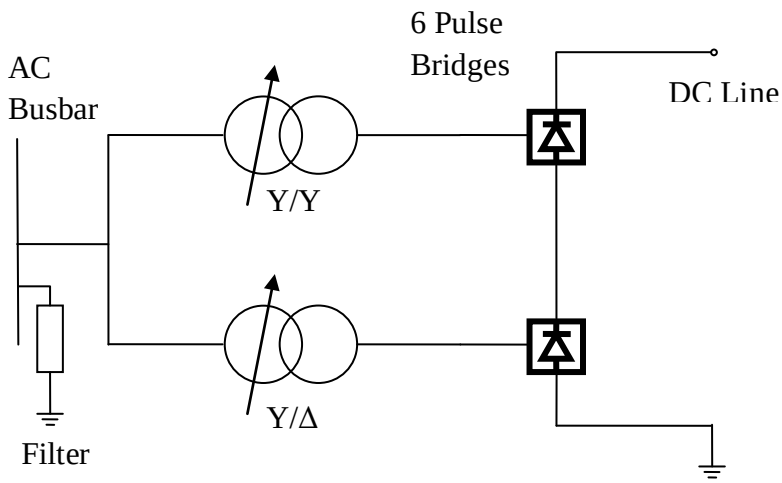

Figure 4 12-Pulse Converter

In deriving the converter equations, it is assumed that the AC system is represented by an ideal voltage source with a constant frequency in series with a lossless inductance (transformer leakage inductance), DC current is constant and ripple free and the valves are ideal with 0 resistance when conducting and infinite resistance when not conducting.

Figure 5 shows the converter operating as a rectifier, Figure 5(a), and operating as an inverter, Figure 5(b). The equivalent circuit in Figure 5(a) will be used for the following analysis. Things to note in Figure 5(a) are the AC line inductance, L_c, which prevents the line current from changing instantaneously and causes commutation overlap which will be discussed. The inductance L_d on the DC side keeps the DC current continuous.

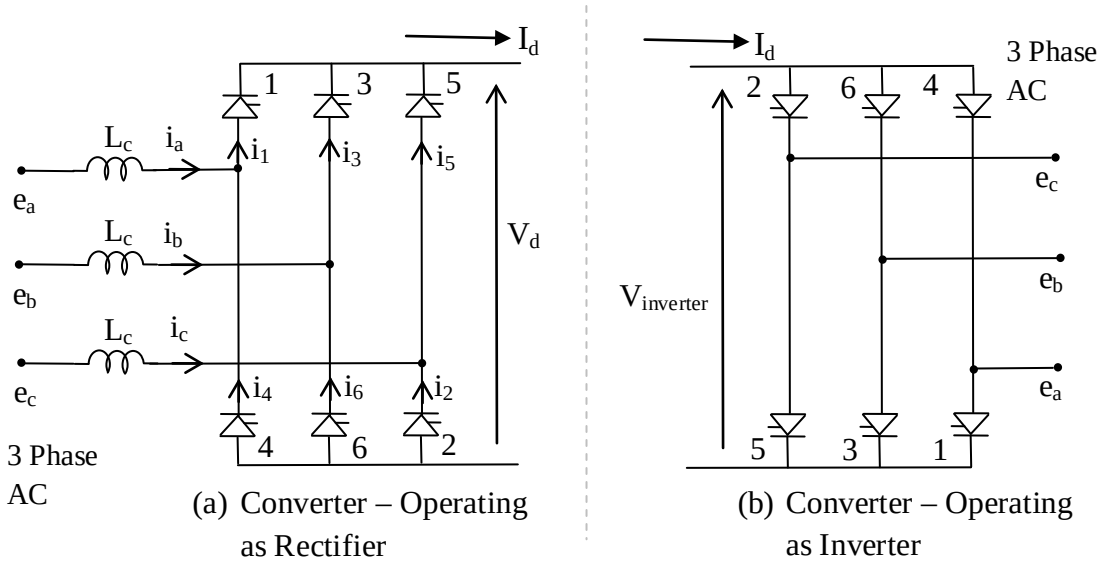

(a) Converter – Operating as Rectifier

(b) Converter – Operating as Inverter

Figure 5 6-Pulse Converter Circuit, [11]

3.2. 2 Rectification, Inversion and Commutation

The converter waveforms under rectification and inversion are shown below in Figures 6 and 7. In Figures 6 and 7, α is the firing angle, μ is the commutation angle and γ is the extinction advance angle. The rectifier equations are stated in terms of the firing angle α and the inverter equations are stated in terms of the extinction advance angle γ. During rectification, the DC voltage, V_d in Figure 5(a), is positive and during inversion the DC voltage is negative to reverse the direction of power flow since current can`t flow in the reverse direction through the valves. Figure 5(b) shows the converter operating as an inverter with the DC voltage V_d being negative and being represented by $V_{inverter}$.

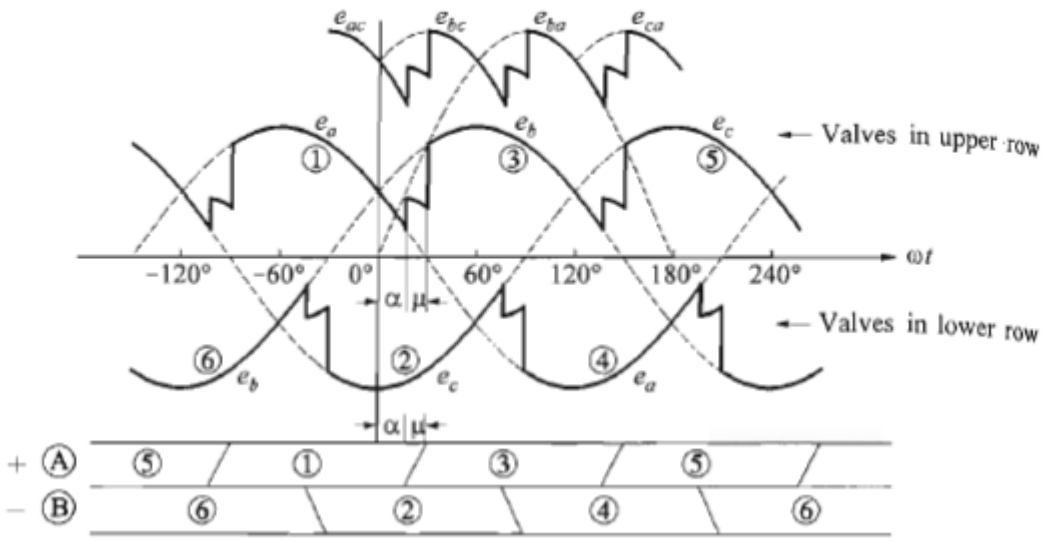

Figure 6 Converter waveforms for rectification, [11]

The waveform in Figure 6 shows the converter operating as a rectifier. The valve firing is delayed for α/ω seconds and the commutation duration, time for the incoming valve to completely pick up the load current, is μ/ω. Thus, after (α+μ)/ω seconds, valve 3 picks up the entire load current.

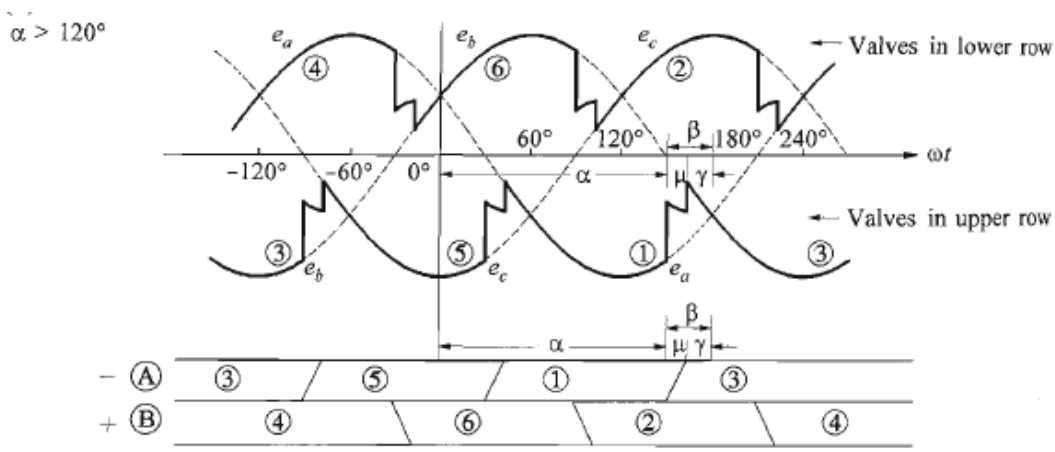

Figure 7 Converter waveforms for inversion, [11]

Current commutation can occur as long as the commutating voltage is positive. Thus waiting for the correct current time and then firing the valve allows the DC voltage polarity to be negative. Figure 7 shows the instance where firing is delayed for an angle of α greater than 120 degrees when e_b is still greater than e_a allowing the conducting valve to switch from 1 to 3. The resulting DC voltage is negative allowing the converter to function as an inverter.

Commutation prevents the immediate rising or falling of the DC current leading to small voltage reductions when converter valves stop and start conducting. When there is no commutation, a firing angle lower than 90° leads to rectification (positive DC voltage) and a firing angle above 90° leads to inversion (negative DC voltage) as shown in Figures 6 and 7. Due to commutation, when current switches from one conducting valve to another, the current rise for the incoming valve and the current fall for the outgoing valve are not instantaneous. This is shown in Figure 8 where the incoming valve 3 picks up the current i_3 and the outgoing valve 1 current i_1 drops over the same duration.

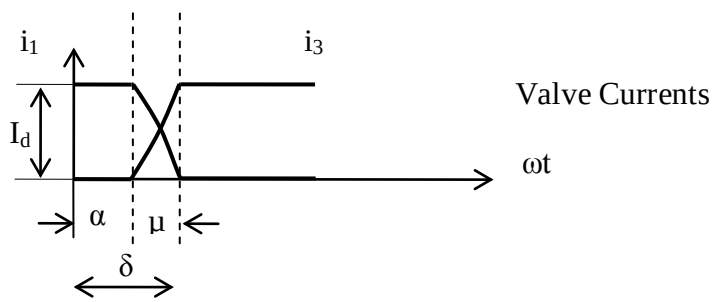

Figure 8 Current commutation, [11]

There must be a limit on the maximum firing angle to allow for proper commutation to occur. The interval after the firing angle has to be long enough so that the commutation voltage is positive during the entirety of the commutation.

3.2.3 AC line current under commutation

If, in Figure 5(a), valve 1 is about to end its conduction period and valve 3 is about to start conducting to pick up the load current, the current in valve 3, i_3, would rise according to equations (3.7) and (3.8), where a is the AC transformer tap, V_c is the AC terminal voltage, X_c is the commutation reactance, α is the firing angle and ω is the line frequency, as given in [10].

$$i_3 = \frac{aV_c}{\sqrt{2}X_c}[cos\alpha - \cos(\omega t)] \tag{3.7}$$

At the end of commutation the angle is $\alpha + \mu$ and the current, i_3, equals the DC load current, I_d, and is given by (3.8), where μ is commutation angle

$$I_d = \frac{aV_c}{\sqrt{2}X_c}[cos\alpha - \cos(\alpha + \mu)] \tag{3.8}$$

3.2.4 DC voltage under commutation

The DC voltage, V_d in Figure 3, is reduced slightly under commutation and is given by (3.9) from [10], where α is the firing angle, μ is the commutation angle and $V_{co} = \frac{3\sqrt{2}}{\pi} aV_c$.

$$V_d = \frac{1}{2}V_{co}[cos\alpha + \cos(\alpha + \mu)] \tag{3.9}$$

Since the commutation angle, μ, is not usually known, we can use the DC current equation (3.8) to rewrite the DC voltage equation (3.9) above so that we have the DC voltage equation in terms of the firing angle and the DC current.

Solving (3.8) for $\cos(\alpha + \mu)$ gives

$$\cos(\alpha + \mu) = cos\alpha - \frac{\sqrt{2}X_c}{aV_c} I_d$$

Substituting the equation above into (3.9) gives the final form of the equation.

$$V_d = \frac{1}{2}V_{co}[cos\alpha + \cos(\alpha + \mu)]$$

$$= \frac{1}{2}V_{co}[cos\alpha + (cos\alpha - \frac{\sqrt{2}X_c}{aV_c} I_d)]$$

$$= V_{co} cos\alpha - \frac{1}{2} V_{co} \frac{\sqrt{2}X_c}{aV_c} \mathrm{I_d}$$

$$= \frac{3\sqrt{2}}{\pi} aV_c cos\alpha - \frac{1}{2} \frac{3\sqrt{2}}{\pi} aV_c \frac{\sqrt{2}X_c}{aV_c} \mathrm{I_d}$$

$$= \frac{3\sqrt{2}}{\pi} aV_c cos\alpha - \frac{3X_c}{\pi} \mathrm{I_d}$$

Hence the DC voltage is also given by (3.10) below. This equation gives the DC voltage in terms of the firing angle and the DC current. The commutation voltage drop is taken account of in this equation by commutation reactance X_c.

$$\mathrm{V_d} = \frac{3\sqrt{2}}{\pi} aV_c cos\alpha - \frac{3X_c}{\pi} \mathrm{I_d} \tag{3.10}$$

3.2.5 Inverter Voltage Equation

If the firing angle is greater than 90 degrees (when there is no commutation) then the DC voltage becomes negative allowing the converter to function as an inverter. The inverter equation is written in terms extinction advance angle γ, due to this angle being the subject of control in inverters. A sufficiently large value of γ is chosen so that commutation can occur safely and the incoming valve can pick up the current. At the same time reactive power consumption increases with a large γ so it should it should not be chosen too large. Typical values found for γ are between 15 to 20 degrees.

The following angles are noted from Figure 7 to write the inverter equations.

$\gamma = \pi - (\alpha + \mu)$

$\beta = \mu + \gamma$

and thus

$\alpha + \beta = \pi$

Writing the current equation, (3.8), using γ and β gives

$\mathrm{I_d} \quad = \frac{aV_c}{\sqrt{2}X_c}[cos\alpha - \cos(\alpha + \mu)]$, from (3.8)

$$= \frac{aV_c}{\sqrt{2}X_c}[\cos(\pi - \beta) - \cos(\pi - \gamma)]$$

$$= \frac{aV_c}{\sqrt{2}X_c}[-\cos\beta + \cos\gamma]$$

Thus, the current equation can be written as

$$I_d = \frac{aV_c}{\sqrt{2}X_c}[-\cos\beta + \cos\gamma] \tag{3.11}$$

Writing the voltage equation, (3.9), using γ and β gives

$$V_d = \frac{1}{2}V_{co}[cos\alpha + \cos(\alpha + \mu)], \text{ from (3.9)}$$

$$= \frac{1}{2}V_{co}[\cos(\pi - \beta) + \cos(\pi - \gamma)]$$

$$= \frac{1}{2}V_{co}[-\cos\beta - \cos\gamma]$$

Thus, the voltage equation can be written as

$$V_d = \frac{1}{2}V_{co}[-\cos\beta - \cos\gamma] \tag{3.12}$$

Solving the current equation (3.11) for cosβ gives

$$\cos\beta = \cos\gamma - \frac{\sqrt{2}X_c}{aV_c}I_d$$

Substituting the equation above into the voltage equation (3.12) gives

$$V_d = \frac{1}{2}V_{co}[-\cos\beta - \cos\gamma]$$

$$= \frac{1}{2}V_{co}[-(\cos\gamma - \frac{\sqrt{2}X_c}{aV_c}I_d) - \cos\gamma]$$

$$= \frac{1}{2}V_{co}[-2\cos\gamma + \frac{\sqrt{2}X_c}{aV_c}I_d]$$

$$= -V_{co}\cos\gamma + \frac{1}{2}V_{co}\frac{\sqrt{2}X_c}{aV_c}I_d$$

$$= -\left(\frac{3\sqrt{2}}{\pi}aV_c\right)(-\cos(\pi - \gamma)) + \frac{1}{2}\left(\frac{3\sqrt{2}}{\pi}aV_c\right)\frac{\sqrt{2}X_c}{aV_c}I_d$$

$$= \frac{3\sqrt{2}}{\pi} aV_c \cos(\pi - \gamma) + \frac{3}{\pi} X_c I_d$$

The final form of the voltage equation for the inverter is given in (3.13).

$$V_d = \frac{3\sqrt{2}}{\pi} aV_c \cos(\pi - \gamma) + \frac{3}{\pi} X_c I_d \tag{3.13}$$

3.2.6 AC Current Fundamental Component (RMS)

Assuming perfect filtering, the AC current is purely sinusoidal. The relationship between the fundamental AC current, I_1, and the DC current I_d is given by (3.14) from Ref. [10]. This equation is derived from Fourier analysis of the square line current waveform and will be useful in simplifying some of the equations.

$$I_1 = \frac{\sqrt{6}}{\pi} I_d \tag{3.14}$$

3.2.7 AC Power Factor - Rectifier

Assuming no power loss over the converter or the transformer, the three phase AC power must equal the DC power leading to the following power equation.

AC power = DC power

$\sqrt{3} aV_c I_1 cos\phi = V_d I_d$

$cos\phi = \frac{V_d I_d}{\sqrt{3} aV_c I_1}$

Substituting V_d and I_d equations (3.9) and (3.14) into the last equation above gives (3.15).

$$\cos\phi = \frac{1}{2}[cos\alpha + \cos(\alpha + \mu)] \tag{3.15}$$

Hence, the phase difference between the fundamental AC voltage and current can be written in terms of the firing angle and the commutation angle. In case of a no commutation (or small commutation) angle, the converter power factor angle is equal to the firing angle.

3.3 Converter Model

The converter equations derived so far can be put in a more succinct form to get the final equations which will serve to model the converter. The equations are derived on the assumption that the AC voltages are balanced and sinusoidal, converter operation is balanced, DC side current and voltage contain no AC components and the converter transformer is lossless and the magnetizing admittance is ignored [10].

The DC variables alluded in equation (3.5) are

$[\bar{x}] = [V_d, I_d, a, cos\alpha, \phi]^T$,

where V_d is the DC voltage, I_d is the DC current, a is the transformer tap, α is the firing angle and ϕ is the phase difference between the converter bus fundamental AC voltage and current. As will be seen in what follows, three of these equations will be determined from 3 independent equations and the other 2 will be taken as control variables which are specified.

3.3.1 DC per unit system

Common voltage and power bases are used on both sides of the converter, i.e. the AC and DC sides. In order to make sure that per unit power on the AC and DC side are the same, the direct current base, gotten from MVA_B/V_B has to be $\sqrt{3}$ times larger than the AC current base [10].

The phase current and DC current relation can be written in per unit as follows next.

The relation between the DC current, I_d, and AC line current given in (3.14) is restated in (3.16) where I_s, Figure 9, represents the transformer secondary side AC current.

$$I_s = \frac{\sqrt{6}}{\pi} I_d, \text{ (from Figure 9 and equation (3.14))} \tag{3.16}$$

Dividing both sides of the above equation by the ac base current and then multiplying and dividing the right side by $\sqrt{3}$ gives the per unit relation in (3.17.a).

$$I_s(pu) = \frac{\sqrt{6}}{\pi}\sqrt{3}I_d(pu) \tag{3.17.a}$$

If commutation overlap is present then the current waveform is not perfectly square and (3.17.a) becomes

$$I_s(pu) = k\frac{\sqrt{6}}{\pi}\sqrt{3}I_d(pu) \tag{3.17.b}$$

where k under normal steady-state operating conditions is above 0.99 [10] and in this thesis k = 1.

With reference to Figure 9, equations (3.18) to (3.22) summarize all the previous converter equations in per unit.

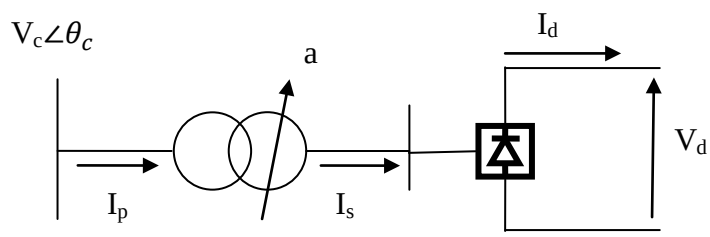

Figure 9 AC Bus, Transformer and Converter

The converter relations in per unit are given in equations (3.18) - (3.22) from reference [10].

The DC per unit equation for AC transformer secondary current, I_s, and DC current, I_d, is given by (3.18).

$$I_s = k\frac{3\sqrt{2}}{\pi}I_d \tag{3.18}$$

The relation for primary transformer current, I_p, and secondary transformer current, I_s, is given in (3.19).

$$I_p = aI_s \tag{3.19}$$

The voltage conversion equation for the converter is given in (3.20) where V_d is the DC voltage, a is the AC transformer tap, V_c is the AC terminal voltage, α is the firing angle, I_d is the DC current and X_c is the commutation reactance.

$$V_d = \frac{3\sqrt{2}}{\pi} a V_c cos\alpha - \frac{3}{\pi} I_d X_c \tag{3.20}$$

Equation (3.21) is based on AC and DC system configurations and will be more fully defined later on.

$$f(V_d, I_d) = 0 \tag{3.21}$$

Assuming no losses, the entirety of the AC power is converted to DC power during rectification and vice versa during inversion as given in (3.22), where V_d and I_d are the DC voltage and current respectively, V_c is the AC terminal voltage, I_p is the AC transformer primary current and ϕ is the power factor angle between the fundamental AC voltage and current.

$$V_d I_d = V_c I_p \cos\phi \tag{3.22}$$

Equation (3.22) can be simplified, using equations (3.18) and (3.19), to eliminate the current values.

$$V_d I_d = V_c I_p \cos\phi$$

Using

$I_s = k\frac{3\sqrt{2}}{\pi} I_d$, from (3.18)

$I_p = aI_s = ak\frac{3\sqrt{2}}{\pi} I_d$, from (3.19)

$$V_d I_d = V_c\left(ak\frac{3\sqrt{2}}{\pi} I_d\right)\cos\phi$$

$$V_d = V_c ak\frac{3\sqrt{2}}{\pi}\cos\phi$$

$$V_d = V_c a k_1 \cos\phi, \text{ where } k_1 = k\frac{3\sqrt{2}}{\pi}$$

Hence, the AC-DC power flow equation (3.22) above is equivalent to equation (3.23).

$$V_d - a k_1 V_c \cos\phi = 0 \tag{3.23}$$

3.3.2 Control Equations

The two required control equations can be any of the following valid controls. The controls are specified and considered as known in the formulation.

1. Specified converter transformer tap

   $$a - a^{sp} = 0 \tag{3.24}$$

2. Specified DC voltage

   $$V_d - V_d^{sp} = 0 \tag{3.25}$$

3. Specified DC current

   $$I_d - I_d^{sp} = 0 \tag{3.26}$$

4. Specified firing angle

   $$\cos\alpha - \cos\alpha_{min} = 0 \tag{3.27}$$

5. Specified DC power to be handled by converter

   $$V_d I_d - P_{DC}^{sp} = 0 \tag{3.28}$$

The DC voltage and the converter firing angle are selected as controls in this work.

3.3.3 Converter Power in terms of the DC System Variables

Q_c(DC) and P_c(DC) in eqns. (3.3) and (3.4) are written in terms of the AC terminal voltage and DC variables.

$$Q_c\,(DC) = V_c I_p \sin\phi$$
$$= V_c a k_1 I_d \sin\phi$$

$$P_c\,(DC) = V_c I_p \cos\phi$$
$$= V_c a k_1 I_d \cos\phi$$
$$\text{OR} = V_d I_d$$

$P_c(DC) = V_c a k_1 I_d \cos\phi$ (3.29)

$Q_c(DC) = V_c a k_1 I_d \sin\phi$ (3.30)

The converter absorbs reactive power whether acting as a rectifier and inverter since the line current lags the voltage. Since by equation (3.13), $\cos\phi = \cos\alpha$ when there is no commutation, and the firing angle α can vary from 0 to 180 degrees, equation (3.28) shows that the converter always absorbs reactive power.

Using the expressions for $P_c(DC)$ and $Q_c(DC)$ from (3.27) and (3.28), equations (3.1) and (3.2) can be written as

$$P_c^{sch} - P_c(AC) - P_c(DC) = P_c^{sch} - V_c \sum_{n=1}^{NB} Y_{cn} V_n \cos(\delta_c - \delta_n - \theta_{cn}) - V_c a_c k_1 I_{d,c} \cos\phi_c = 0$$

$$Q_c^{sch} - Q_c(AC) - Q_c(DC) = Q_c^{sch} - V_c \sum_{n=1}^{NB} Y_{cn} V_n \sin(\delta_c - \delta_n - \theta_{cn}) - V_c a_c k_1 I_{d,c} \sin\phi_c = 0$$

$$P_c^{sch} = V_c \sum_{n=1}^{NB} Y_{cn} V_n \cos(\delta_c - \delta_n - \theta_{cn}) + V_c a_c k_1 I_{d,c} \cos\phi_c \quad (3.1.a)$$

$$Q_c^{sch} = V_c \sum_{n=1}^{NB} Y_{cn} V_n \sin(\delta_c - \delta_n - \theta_{cn}) + V_c a_c k_1 I_{d,c} \sin\phi_c \quad (3.2.a)$$

3.3.4 Summary

The equations necessary to incorporate converters into load flow were derived in this chapter. The final form of the equations is given below in equations (3.31) to (3.35).

In summary, each converter (rectifier/inverter) has 3 unknowns and 3 equations and 2 control equations which fix two variables.

$R(1) = V_d - a k_1 V_c \cos\phi = 0$ (3.31)

$R(2) = V_d - \frac{3\sqrt{2}}{\pi} a V_c \cos\alpha + \frac{3}{\pi} I_d X_c = 0$ (3.32.a)

Or

$R(2) = V_d - \frac{3\sqrt{2}}{\pi} a V_c \cos(\pi - \gamma) - \frac{3}{\pi} I_d X_c = 0$ (3.32.b)

$R(3) = f(V_d, I_d) = V_d I_d - P_{DC} = 0$ (3.33)

$R(4) = \text{control equation} = V_d - V_d^{sp} = 0$ (3.34)

$R(5) = \text{control equation} = \cos\alpha - \cos\alpha^{sp} = 0$ (3.35.a)

Or

$R(5) = \text{control equation} = \cos(\pi - \gamma) - \cos(\pi - \gamma^{sp}) = 0$ (3.35.b)

Equation R(2) has 2 forms, the first form is used for a rectifier and the second form is used for an inverter. The first form of R(2) being for a rectifier has positive converter DC voltage, V_d, and the second form being for an inverter has negative DC voltage, V_d. The reason for the different forms of the voltage equation is that the firing angle, α, is usually taken as the control angle for a rectifier and the extinction advance angle, γ, is taken as the control for an inverter and these are explicitly represented in the two forms of the equation. The proper equation R(5) has to be chosen based on whether the converter is a rectifier or an inverter.

The unknowns in this thesis are taken to be the transformer tap (a), the DC current (I_d) and the converter power factor angle (ϕ) and the controls are taken to be the converter firing angle (α) (extinction advance angle, γ, if converter is an inverter) and the DC voltage (V_d). Equation R(3) is chosen such that the converter power $V_d I_d$ is injected into the DC system.

Chapter 4: AC-DC OPF Problem Formulation

The Microgrid 24 hour scheduling problem is formulated as a mixed-integer nonlinear programming (MINLP) problem where the total cost of supplying the load is minimized. This is similar to the traditional OPF problem but in this case, the network is more complicated than a typical AC network; the Microgrid load flow takes account of the AC network, the DC network and also the converters. The problem objective is to schedule the Microgrid over 24 hours such that the cost of supplying the load is a minimum. The objective is also to ensure that the optimal schedule is reliable by storing energy required for the next few hours in the available storage devices in the Microgrid. The most important costs are the cost of Microgrid generation, represented by a quadratic cost function, the cost of energy import from the Microgrid and the battery charging cycle cost. The battery charging cycle cost is much smaller compared to the other costs. The objective functions and the constraining equations are given in this chapter.

4.1 Problem Formulation

Two objectives are considered. The first objective, given in Section 4.1.1, schedules the Microgrid so that the loads are satisfied at minimum cost and thus involves only one objective function. The second objective, given in Section 4.1.2, schedules the Microgrid so that not only are the loads satisfied at minimum cost but also that the Microgrid reliability is maintained at a high level and thus involves two objectives functions which are handled via a Fuzzy optimization formulation.

4.1.1 Economic Objective

The first objective considers a purely economic problem where the objective is to minimize the cost of supplying the load.

Economic Objective:

The economic objective seeks to minimize the cost of supplying the load. The costs considered are the AC generation cost, the cost of importing power into the Microgrid and finally the battery charge cycle cost. The objective is shown in (4.1) where t is the time index, i is the generator index, a_i, b_i and c_i are the quadratic cost coefficients for the AC generators, $PG_{i,t}$ is the AC power generation by generator i at time t, $P_{import,t}$ is the real-time price for importing power from the overlying grid, CC is the battery charge cycle cost (taken to be negligible) and S_t is a binary variable indicating the starting of a charge cycle.

Min Cost: $\sum_{t=1}^{NT}[\sum_{i=1}^{NG}\left(a_i PG_{i,t}^2 + b_i PG_{i,t} + c_i\right) + P_{import,t} * MP_t + CC * S_t]$ (4.1)

4.1.2 Dual Objectives - Economic and Reliability Objectives

The second objective is a dual objective where both economic and reliability considerations are taken into account. The goal here is to minimize costs given by (4.1) and also maximize reliability which is defined as follows.

In order to evaluate reliability, a reliability index (RI) is defined to compare the energy stored in the battery to the total real power load at a certain time. More precisely, the reliability index is defined as the minimum of the hourly stored energy in the battery to the total hourly real power load ratio over the hours of operation as in (4.2) where tn varies over the time index, BPC_t is the battery charging at time t, BPD_t is the battery discharging at time t and $TotalLoad_{tn}$ is the total load at time tn.

$$\mathrm{RI} = \min_{\forall \mathrm{tn}} \left\{ \frac{\sum_{t=1}^{\mathrm{tn}} (\mathrm{BPC_t} - \mathrm{BPD_t})}{\mathrm{TotalLoad_{tn}}} \right\} \quad (4.2)$$

$\forall \mathrm{tn} = 1, \dots, \mathrm{NT}$

The reliability index values will range from 0 to above indicating if the energy stored in the battery is sufficient to cover the load if the need arises. If the battery holds no energy, the RI will be 0 and if the battery holds energy equal to the load then RI will be 1 and so on.

If the objective is the minimization of cost given in (4.1) and maximization of reliability given in (4.2) then these are contradictory objectives since a greater reliability requirement will

lead to the battery holding more energy at all times and thus costs would increase. To deal with the dual contradictory objectives, fuzzy optimization is used.

1. Fuzzy Model of Cost Minimization Objective

The fuzzy set for cost is defined as

$$Cost_set = \{ (Cost, \mu c) \mid Cost_{min} < Cost\ (PG, P_{import,} S) < Cost_{max} \} \quad (4.3)$$

In (4.3), μc is the fuzzy satisfaction function for cost, $Cost_{min}$ and $Cost_{max}$ are the minimum and maximum costs and Cost (PG, $P_{import,}$ S) is the cost of satisfying the load.

The satisfaction function of the cost fuzzy set is

$$\mu c = \frac{Cost_{max} - Cost(PG, P_{import}, S)}{Cost_{max} - Cost_{min}} \quad (4.4)$$

, where $COST_{min}$ is taken to be the minimum cost required to satisfy the load when no reserve is required to be held and $COST_{max}$ is taken to be the maximum cost required when the most expensive generators are used to supply the load as well as to charge the battery up to capacity. The satisfaction function takes on the value μc = 1 when the cost given in (4.1), $Cost(PG, P_{import}, S)$, is minimum and takes on the value μc = 0 when the cost is maximum.

2. Fuzzy Model of Reliability Maximization Objective

In order to maximize reliability, the battery should hold the most amount of energy possible in the battery at any time which will lead to a high RI as given in (4.2).

The fuzzy set for energy is defined as

$$TEB_set_t = \{ (TEB, \mu e_t) \mid TEB_{min} < TEB_t < TEB_{max} \} \quad (4.5)$$

In (4.5), μe_t is the fuzzy satisfaction function for the energy stored in the battery, TEB is the total energy stored in the battery, TEB_{min} and TEB_{max} are chosen as the minimum and the maximum energy stored in the battery.

The satisfaction function of the energy fuzzy set is

$$\mu e_t = \frac{TEB_t - TEB_{min}}{TEB_{max} - TEB_{min}} \quad (4.6)$$

, where TEB_{max} and TEB_{min} are chosen as equal to the battery capacity and 0. When the energy stored in the battery is maximum then $\mu e_t = 1$, indicating maximum satisfaction, and when the energy stored in the battery is minimum then $\mu e_t = 0$.

Fuzzy optimization maximizes the minimum of all the satisfaction parameters where λ is defined as the minimum of all the satisfaction functions. Hence, (4.4) and (4.6) take the form in (4.7) and (4.8).

$$\lambda \leq \mu c = \frac{Cost_{max} - Cost(PG, P_{import}, S)}{Cost_{max} - Cost_{min}} \tag{4.7}$$

$$\lambda \leq \mu e_t = \frac{TEB - TEB_{min}}{TEB_{max} - TEB_{min}} \tag{4.8}$$

Thus, the fuzzy optimization objective is

$$\text{Maximize } \lambda = \min\{ \mu c, \mu e_1, \ldots, \mu e_{NT} \} \tag{4.9}$$

Maximizing λ forces the solution towards minimum cost and maximum energy held in the battery.

The constraining equations that are common to both objectives will now be given. The constraining equations can be separated into the AC network equations, the DC network equations and the converter equations. The AC network equations are the typical equations found in any OPF problem. The DC network equations, much like the AC power flow equations ensure that the power balance is achieved in the DC network at all nodes. The converter equations govern the converter behaviour so that the AC and DC networks can exchange power.

4.2 AC Network Equations

4.2.1 AC Generator Equations

Real power balance equations are needed at all generator buses. Any grid power import buses are also treated as a generator buses but they are given separately for emphasis. In equation (4.10), $PG_{k,t}$ is the power generation at the kth generator bus at time t, $PD_{k,t}$ is the power demand at the kth bus at time t, $V_{k,t}$ is the voltage at the kth generator bus at time t, Y_{kn} is the AC admittance

matrix entry magnitude, $\delta_{k,t}$ is the voltage angle for the kth generator bus at time t and $\theta_{kn}$is the AC admittance matrix entry angle.

$$P_{k,t} = PG_{k,t} - PD_{k,t} = V_{k,t} \sum_{n=1}^{NB} Y_{kn} V_{n,t} \cos(\delta_{k,t} - \delta_{n,t} - \theta_{kn}) \quad (4.10)$$

$\forall k =$ all AC generator buses

$\forall t$ = 1,…,NT

4.2.2 Load Bus Equations

The load bus equations, (4.11) and (4.12), ensure that load demands are met at each load bus.

$$P_{k,t} = -PD_{k,t} = V_{k,t} \sum_{n=1}^{NB} Y_{kn} V_{n,t} \cos(\delta_{k,t} - \delta_{n,t} - \theta_{kn}) \quad (4.11)$$

$$Q_{k,t} = -QD_{k,t} = V_{k,t} \sum_{n=1}^{NB} Y_{kn} V_{n,t} \sin(\delta_{k,t} - \delta_{n,t} - \theta_{kn}) \quad (4.12)$$

$\forall k$ = all AC load buses but excluding any buses connected to converters

$\forall t$ = 1,…,NT

4.2.3 Power Import Bus Equations

Power is imported from the grid into the Microgrid. This bus is treated as a generator with the price of power purchase being the market price. Equation (4.13) gives the equation to be satisfied at the power import bus.

$$P_{k,t} = P_{import,k,t} - PD_{k,t} = V_{k,t} \sum_{n=1}^{NB} Y_{kn} V_{n,t} \cos(\delta_{k,t} - \delta_{n,t} - \theta_{kn}) \quad (4.13)$$

$\forall k$ = all AC power import buses connected to the grid

$\forall t = 1, \dots, NT$

4.2.4 Converter Bus Equations

$$P_{c,t} = P_{c,t}(AC) + P_{c,t}(DC) \quad (4.14)$$

$Q_{c,t} = Q_{c,t}(AC) + Q_{c,t}(DC)$ (4.15)

Using equations (3.1.a) and (3.2.a), equations (4.14) and (4.15) can be written as the power flow equations at the converter buses.

$P_{c,t} = V_{c,t} \sum_{n=1}^{NB} Y_{cn} V_{n,t} \cos(\delta_{c,t} - \delta_{n,t} - \theta_{cn}) + V_{c,t} a_{c,t} k_1 I_{d,c,t} \cos\phi_{c,t}$ (4.16)

$Q_{c,t} = V_{c,t} \sum_{n=1}^{NB} Y_{cn} V_{n,t} \sin(\delta_{c,t} - \delta_{n,t} - \theta_{cn}) + V_{c,t} a_{c,t} k_1 I_{d,c,t} \sin\phi_{c,t}$ (4.17)

$\forall c$ = all AC buses connected to converters

$\forall t = 1,\ldots,NT$

4.3 Converter Equations

Each converter has 3 unknowns and thus 3 equations are needed to incorporate the converters into load flow. The first equation is derived from AC power flow, the second equation is the voltage conversion equation and the third equation is derived from DC power flow. There are two additional equations which serve as control equations for the converter. The equations, as given and explained in Chapter 3, equations (3.29)-(3.33), are given below as equations (4.18)-(4.22) incorporating the time index t.

$R_{c,t}(1) = V_{d,c,t} - a_{c,t} k_1 V_{c,t} \cos\phi_{c,t} = 0$ (4.18)

$R_{c,t}(2) = V_{d,c,t} - \frac{3\sqrt{2}}{\pi} a_{c,t} V_{c,t} \cos\alpha_{c,t} + \frac{3}{\pi} I_{d,c,t} X_c = 0$

OR

$R_{c,t}(2) = V_{d,c,t} - \frac{3\sqrt{2}}{\pi} a_{c,t} V_{c,t} \cos(\pi - \gamma_{c,t}) - \frac{3}{\pi} I_{d,c,t} X_c = 0$ (4.19)

$R_{c,t}(3) = f(V_d, I_d) = V_{d,c,t} I_{d,c,t} - V_{dc,c,t} (\sum_{n=1}^{N} Y_{dc,cn} V_{dc,n,t}) = 0$ (4.20)

$R_{c,t}(4) = V_{d,c,t} - V_{d,c}^{sp} = 0$ (4.21)

$R_{c,t}(5) = \alpha_{c,t} - \alpha_c^{sp} = 0$

OR

$R_{c,t}(5) = \gamma_{c,t} - \gamma_c^{sp} = 0$ (4.22)

$\forall c$ = all buses connected to converters

$\forall t = 1,\ldots,NT$

R(3) is a nodal power equation for the DC system. The converter power is injected into the DC system node.

$V_{d,c,t}$ *– Converter DC voltage for the converter at AC bus c at time t*

$I_{d,c,t}$ *- Converter DC current for the converter at AC bus c at time t*

$a_{c,t}$ *– Transformer tap for the converter at AC bus c at time t*

$V_{dc,n,t}$ *- DC voltage at DC system node n (Note:* $V_{dc,n,t} = |V_{d,c,t}|$ *if the* n^{th} *DC bus is connected to converter c. The absolute value is taken because the DC bus is connected to the positive terminal of the converter.)*

V_c *- AC terminal voltage at converter*

4.4 DC Network Equations

The DC power flow equations make sure that power balance is achieved at each bus of the network.

4.4.1 DC Load Buses

The relation between the power injection into the DC network k^{th} bus at time t and the DC voltage at that bus must satisfy equation (4.23), where $P_{dc,k,t}^{sch}$ is the scheduled DC power injection at the kth DC bus at time t, $V_{dc,k,t}$ is the DC voltage at the kth bus at time t and $Y_{dc,kn}$ is the DC network admittance matrix entry for the connection between bus k and n.

$P_{dc,k,t}^{sch} = V_{dc,k,t}(\sum_{n=1}^{NDC} Y_{dc,kn} V_{dc,n,t})$ (4.23)

$\forall k = 1,\ldots,NDC$ (number of DC buses)

$\forall t = 1,\ldots,NT$

4.4.2 DC Buses that have a Battery

A battery discharge is treated a power injection into the DC network at the battery bus and when the battery charges, it is taken as a load. In (4.24), $BPD_{k,\,t}$ and $BPC_{k,\,t}$ are the battery discharges and charges respectively, $V_{dc,\,k,\,t}$ is the DC voltage at the kth bus at time t and $Y_{dc,\,kn}$ is the DC network admittance matrix entry for the connection between buses k and n.

$$BPD_t - BPC_t = V_{dc,k,\,t}\left(\sum_{n=1}^{NDC} Y_{dc,kn} V_{dc,n,t}\right) \tag{4.24}$$

$\forall k$ = DC network bus connected to a battery (assuming only one battery is present and this is the case examined in this thesis)

$\forall t$ = 1,…,NT

4.4.3 DC Converter buses

The equations for DC buses that have power converters attaching them to the AC network have been taken account of in the converter equations $R_{c,\,t}(3)$ in (4.20). The power flow through the converters must match the power flow through the DC network bus.

4.4.3 DC Buses that have a PV Array

The PV array forecast is assumed to be known and PV production is injected into the DC network to which the PV array is connected. In (4.25), $PV_{k,\,t}^{sch}$ is the PV array power injection into the DC network by the PV array at bus k, $V_{dc,k,\,t}$ is the DC voltage at the kth DC network bus and $Y_{dc,\,kn}$ is the DC network admittance matrix entry for the connection between buses k and n.

$$PV_{k,\,t}^{sch} = V_{dc,k,\,t}\left(\sum_{n=1}^{NDC} Y_{dc,kn} V_{dc,n,t}\right) \tag{4.25}$$

$\forall k$ = 1,…,NPV (number of PV array buses)

$\forall t$ = 1,…,NT

4.4.4 Battery Equations

The battery charging and discharging are limited by (4.26) and (4.27) where BPD_t and BPC_t are the battery charging and discharging respectively, BPDUPPER and BPCUPPER are the upper limits placed on the charging and discharging powers and UPD_t and UPC_t are binary variables indicating if the battery is discharging or charging during time t.

$$BPD_t \leq BPDUPPER*UPD_t \tag{4.26}$$

$$BPC_t \leq BPCUPPER*UPC_t \tag{4.27}$$

$\forall t = 1,\ldots,NT$

The battery can either be charging or discharging at time t and S_t is a binary variable in indicating if a charging cycle starts at time t leading to

$$UPC_t + UPD_t \leq 1 \tag{4.28}$$

and

$$S_t = \max(UPC_t - UPC_{t-1}, 0) \tag{4.29}$$

$\forall t = 1,\ldots,NT$

If the battery is required to act as a reserve then the energy stored in the battery depends not only on the stored energy but also on the required reserve

$$RESERVE_t \leq \sum_{t=1}^{tn}(PC_t - PD_t)*1Hr \leq BATTERYCAPACITY \tag{4.30}$$

$\forall tn = 1, \ldots, NT$

$RESERVE_t$ is reserve energy required in the battery at time t.

4.5 Summary – Complete Formulation

There are two objectives which were discussed in this chapter. The first objective is stated in Section 4.1.1 looks at finding a minimum cost, equation (4.1), solution to satisfy the load demand. The costs taken account of are given in equation (4.1) and include the AC

generation cost, the power import cost and the battery charge cycle cost. The solution is subject to the AC power flow equations (4.10) - (4.17), the converter equations (4.18) - (4.22), the DC power flow equations (4.23) - (4.25) and finally the battery equations (4.26) - (4.30). The AC power flow and DC power flow equations ensure that power balance is achieved at each bus of the network while the converter equations ensure the correct power transfer between the two networks and finally the battery equations place limit on the battery capacity as well as battery charging and discharging among other things.

The complete formulation for minimum cost objective takes the form below, where the equation numbers correspond to the numbers given to these equations in this chapter.

Minimize Cost:

Cost = $\sum_{t=1}^{NT}[\sum_{i=1}^{NG}(a_i PG_{i,t}^2 + b_i PG_{i,t} + c_i) + P_{import,t} * MP_t + CC * S_t]$ **(4.1)**

Subject to:

AC Power Flow Equations	**(4.10) – (4.17)**
Converter Equations	**(4.18) – (4.22)**
DC Power Flow equations	**(4.23) – (4.25)**
Battery Equations	**(4.26) – (4.30)**

The second objective examined is given in (4.9) where the dual objective problem of minimizing cost and maximizing the energy stored in the battery is modeled as a fuzzy problem. The constraining equations for this objective involve equations (4.7) and (4.8) which are the Fuzzy model of cost minimization and Fuzzy model of reliability maximization respectively. The rest of the constraining equations are the same as the first objective discussed above.

The complete formulation is stated below where the equation numbers correspond to the numbers given to these equations in this chapter.

Maximize λ:

$$\lambda = \min\{ \mu c, \mu e_{1,\ldots,} \mu e_{NT}\} \quad (4.9)$$

Subject to:

Fuzzy Model Constraints	**(4.7) – (4.8)**
AC Power Flow Equations	**(4.10) – (4.17)**
Converter Equations	**(4.18) – (4.22)**
DC Power Flow equations	**(4.23) – (4.25)**
Battery Equations	**(4.26) – (4.30)**

The above is set up and solved for a Microgrid using a non-linear programming solver (AIMMS v.3.11 programming environment using KNITRO as the solver) to determine the optimal schedule. The case study and results are discussed in the next chapter.

Chapter 5: Test Case and Results

The results for the two formulations presented in Chapter 4 are given in this chapter. The Microgrid topology and data used are given first, Sections 5.1-5.2 and then the results are analyzed in Sections 5.3-5.6. The first case examined in the minimum cost scheduling of the Microgrid in Sections 5.3-5.5 and the second case examined is the minimum cost and maximum reliability scheduling in Section 5.6.

5.1 Test Case Microgrid

The test case Microgrid, having the general topology as shown in Figure 1, consists of two separate networks, one is an AC network and the other is a DC network, that are interconnected by a set of bi-directional converters. The AC network of the Microgrid is also connected to the external utility grid to import power whenever the market price favours importing rather than local production. The AC and DC Microgrid components are connected together using power converters.

5.1.1 AC Network Components

The AC network taken is a 14-bus IEEE network, Figure 10, altered slightly by removing the generator at bus 6. The network contains conventional small scale generation to supply the Microgrid. The AC network component of the Microgrid has 3 connections which allow it to transfer power into and out of the AC component of the Microgrid. The AC component of the Microgrid is connected to the external utility grid which allows it to import power whenever it is more convenient than generating power locally and this is represented by the generator at bus 8. The AC component of the Microgrid is also connected to the DC component of the Microgrid at 2 buses using power converters. One converter acts strictly as a rectifier transferring power from AC system bus 12 to DC system bus 2 and the 2nd converter acts strictly as an inverter transferring power from DC system bus 4 to AC system bus 13. The generator data, transformer

data and load are given in Appendix A in the Generator Data table, Transformer Data table, Transmission Line Data, P Load Data and Q Load Data tables respectively.

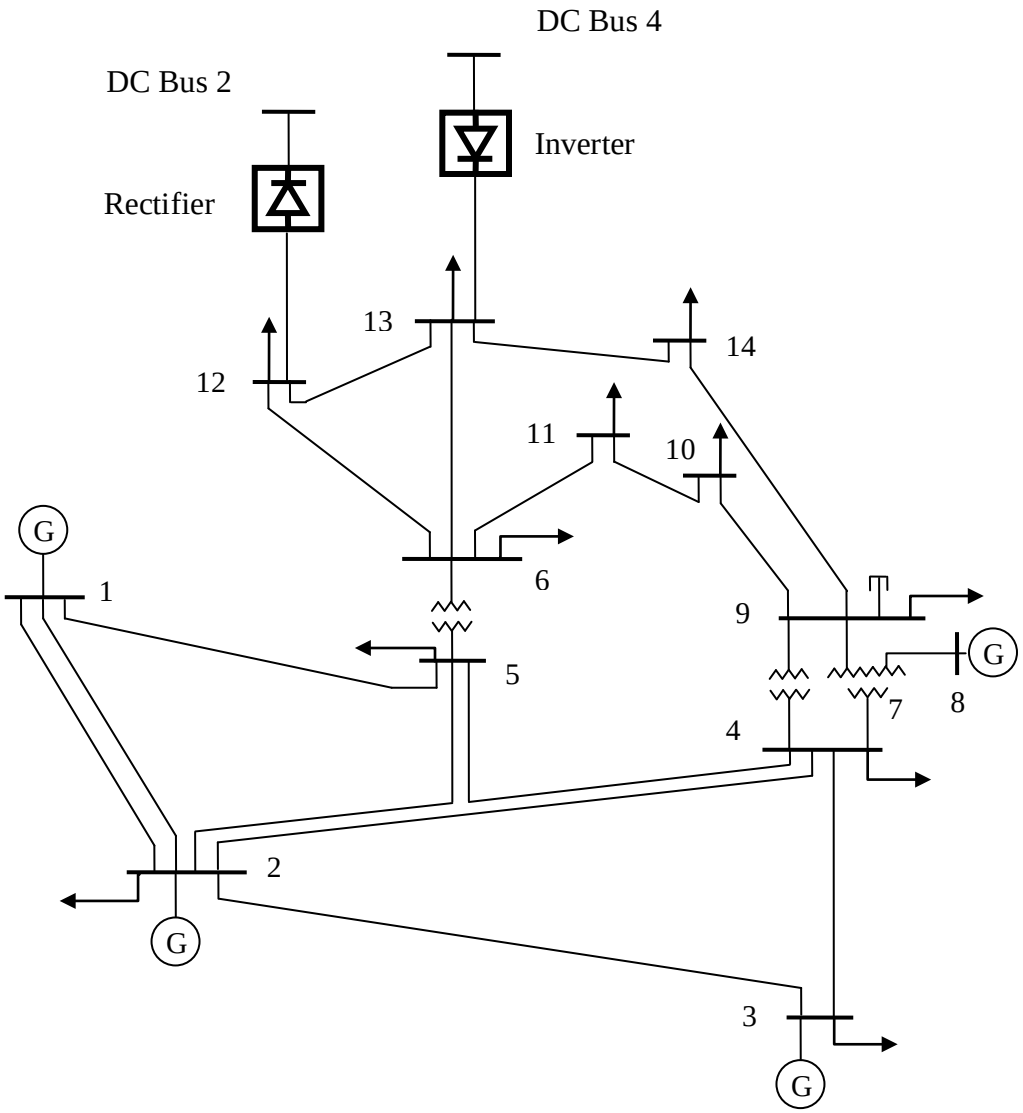

Figure 10 IEEE 14 Bus slightly altered

5.1.2 DC Network Components

The DC components of the Microgrid consist of a PV array, a battery and a DC load which are directly connected to the Microgrid. Any other components, such as a fuel cell can

also be connected directly to the DC grid using DC-DC converters to interface with the network at the DC network voltage. According to the system components, the DC component is primarily responsible for renewable penetration into the Microgrid and storage. The DC network topology is shown in the Figure 11.

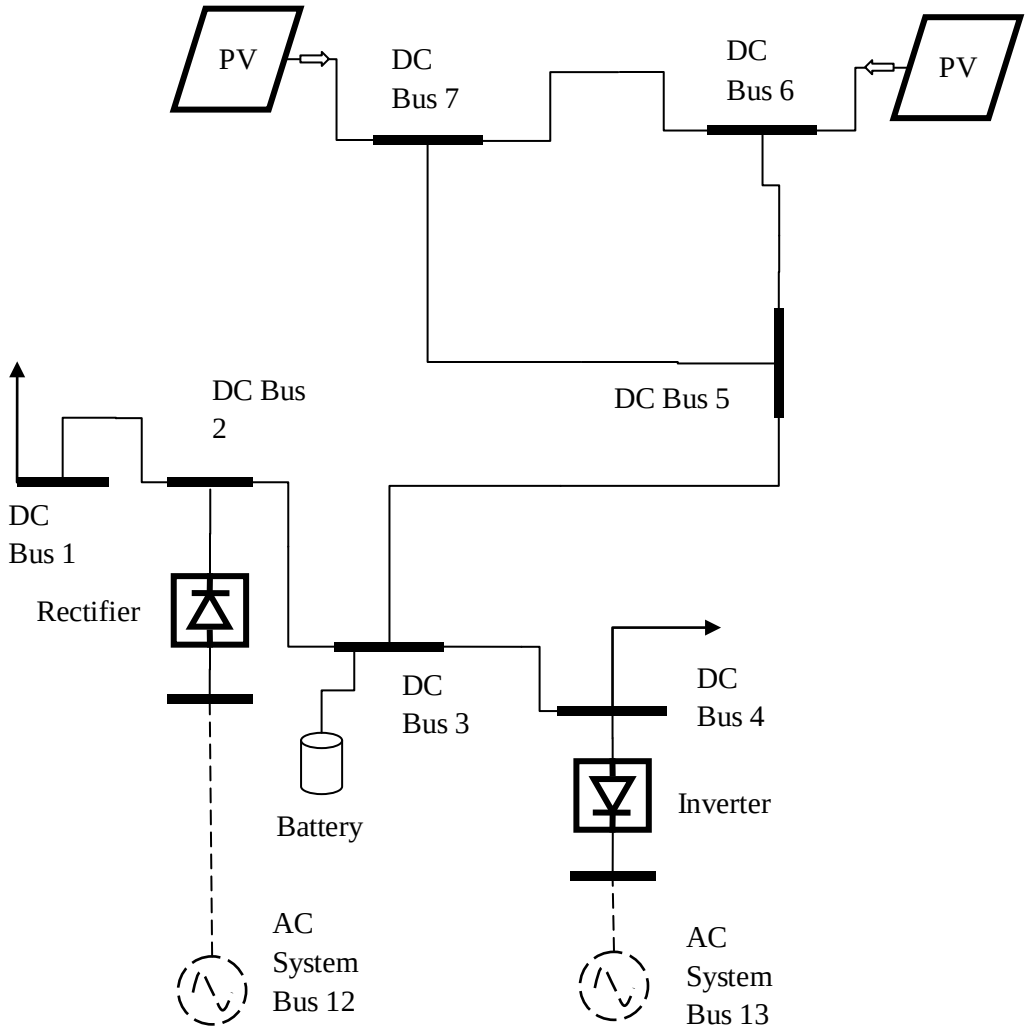

Figure 11 Microgrid DC System

One benefit of this separation of the AC and DC components is that any regulations concerning power converters and their connection to the grids can be localized whereas multiple converters

connected throughout the Microgrid would require additional filtering components to ensure harmonic regulations are met.

5.2 Test-Case (Microgrid with 14 Bus AC system and 7 bus DC system)

5.2.1 AC System

The 24-hr energy demand of the Microgrid is approx. 3 MWh with the average hourly energy demand of around 130 kWh (exact network and load data is in the Appendix A). In order to ensure that local generation can satisfy this demand without relying on the external grid, battery or PV, the Microgrid contains 3 generators with sufficient ratings to satisfy the local Microgrid demand. A connection to the utility grid, at bus 8, is also present in case the generation is not enough or if a generator goes down and allows the Microgrid to import power. There is an upper limit, 10 kW, placed on the power import from the grid under normal operations to ensure that the Microgrid is as self-sufficient as possible. Generator 3 is rated much higher than either of the 2 other generators just for security and reliability measures in case no power can be imported from the utility grid. Also, in case the battery is required to act as a reserve and support the load for a few hours ahead then generator 3 is mainly responsible for providing the energy for the battery while the other two generators support the instantaneous load. The cost functions for the generators are shown in Table 1. Only these costs are considered and start up and shutdown costs, ramp rate limits etc. are ignored to keep things simple and also because two the generators are very small.

Table 1: Generator Cost Functions

Generator	**Ratings**	**Cost Function ($)**
1	40 kW	$0.02PG^2 + 20.1PG + 1.4$
2	50 kW	$0.02PG^2 + 20.15PG + 1.3$
3`	650 kW	$0.02PG^2 + 20.25PG + 1.25$

5.2.2 DC System

The Microgrid DC component contains two PV arrays, one rated at 10 kW and the other rated at 25 kW. The energy forecast for the two PV arrays is assumed to be completely known. The battery located in the system provides system security by acting as a reserve when needed. Specific cases for the battery acting as a reserve are considered where the battery is required to hold enough energy to support the entire load for 1, 2, 3 and 4 hrs ahead. Since the total life a battery is directly linked to the number of charging and discharging cycles, there is a cost associated with a battery on a per charge cycle basis [18]. It is assumed in this formulation that the battery cost is extremely small. DC buses 2 and 4, Figure 11, are connected to the DC system via the rectifier at DC bus 2 and the Inverter at DC bus 4. The DC load data and DC network data are given in Appendix B in the DC Load Data table and DC Network Line Resistance table respectively.

5.2.3 Converters

As already stated in Chapter 3, the unknowns in this thesis are taken to be the transformer tap (a), the DC current (I_d) and the power factor angle (ϕ) and the controls are taken to be the converter firing angle (α) (extinction advance angle, γ, if converter is an inverter) and the DC voltage (V_d). The control data is given in Table 2. The voltage at the converters sets the voltage for the DC network and it is taken arbitrarily. If desired, the operating voltage of the DC network can be much different from the AC network. The voltages at all other DC buses are solved for in the load flow to satisfy equations (4.23)-(4.25).

Table 2: Converter Controls

DC Bus	**Control Angle (Degrees)**	**Control Voltage (pu)**
2	15	1.05
4	15	1.04

5.2.3 System Load Data, PV Forecast and Market Price

The total real power demand of the Microgrid for each hour is shown in Figure 12. This includes the real power demand of the AC network as well as the DC network. The power demand for the system peaks during t = 17 – 22 h. The PV forecast for the two PV arrays is shown in Figure 13.

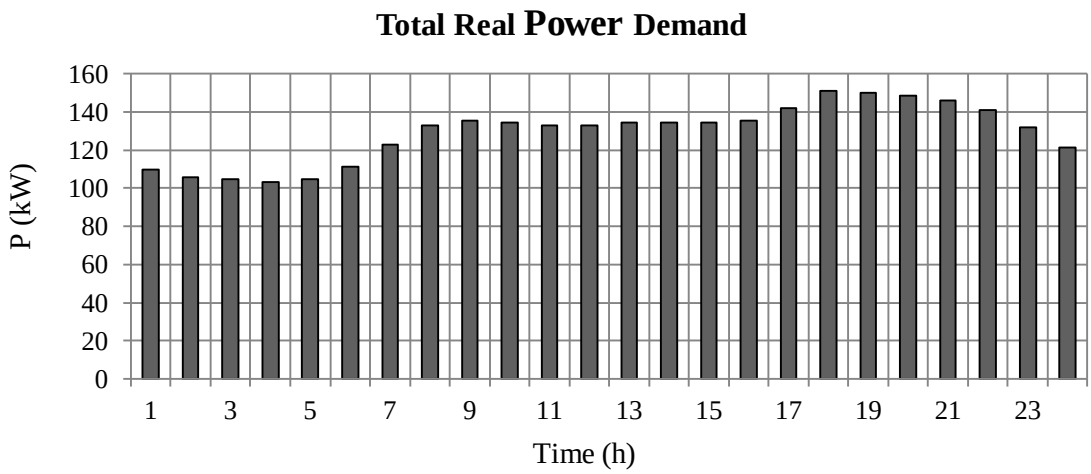

Figure 12 Total Real Power Demand

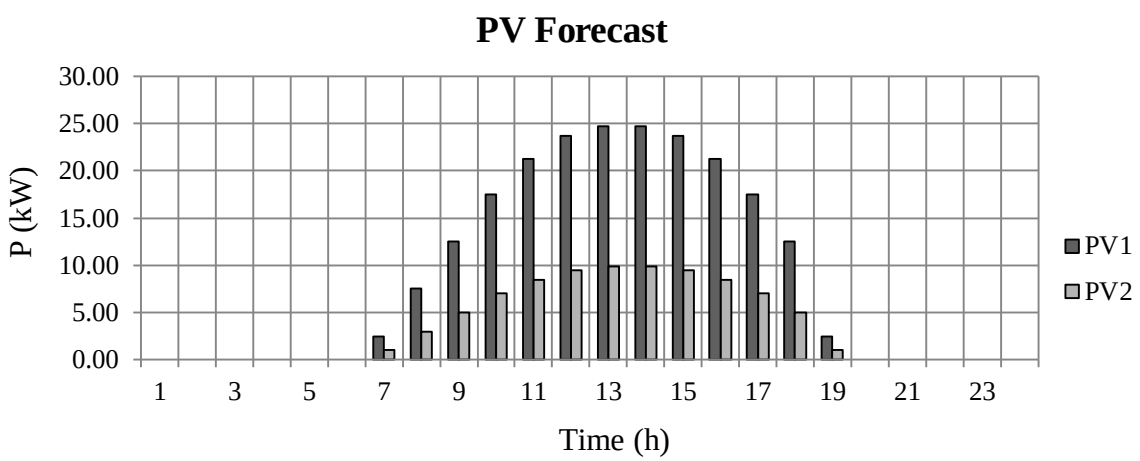

Figure 13 PV Arrays Production Forecast

The two PV arrays are assumed to be located in the same place and have similar production profiles but the ratings of the two arrays are different. The PV array peak output occurs before peak load so the PV energy could better be utilized if it was shifted to a few hours after and this exact role is played by the battery which is located at DC bus 3.

The market price, which is the basis for making decisions regarding importing power from the grid, is shown in Figure 14.

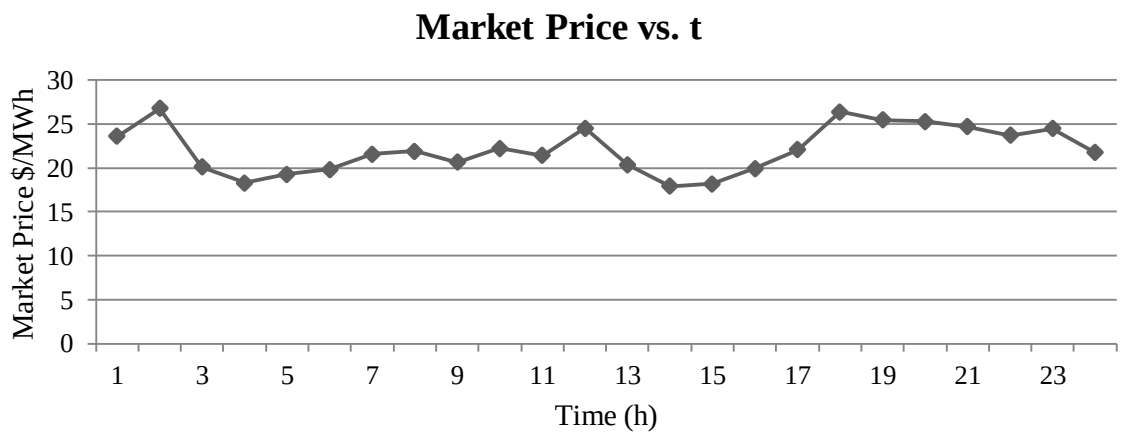

Figure 14 Market Price

The AC and DC load data comprising Figure 12 can be found in Appendix A in the P Load Data table and in Appendix B in the DC Load Data table respectively. The market price numerical data can be found in Appendix A in the Market Price table.

5.3 Results (No Reserve)

The first case to consider is the case when the battery is not required to hold any reserve. The network nodal voltage solution is given in Appendix D for the no reserve case. Figure 15 shows the generator schedule for the 24 hrs. Generators 1 and 2 being the least expensive are used to their full potential and generator 3, acting as the load following generator, supplies the rest.

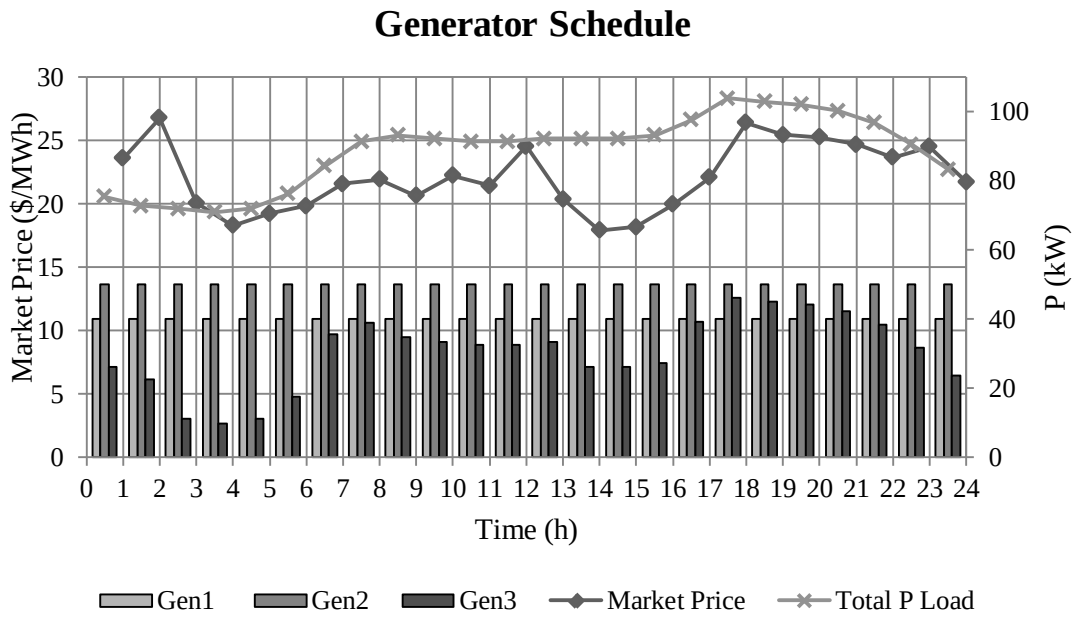

Figure 15 Generator Schedule

Figures 16 shows the battery schedule during power import from the grid and Figure 17 shows PV array power production. Power is imported whenever the market price is cheaper than the Microgrid generation cost. The battery charging occurs during the power import and PV array production times as can be seen by noting the graphs between t = 10 - 17 h.

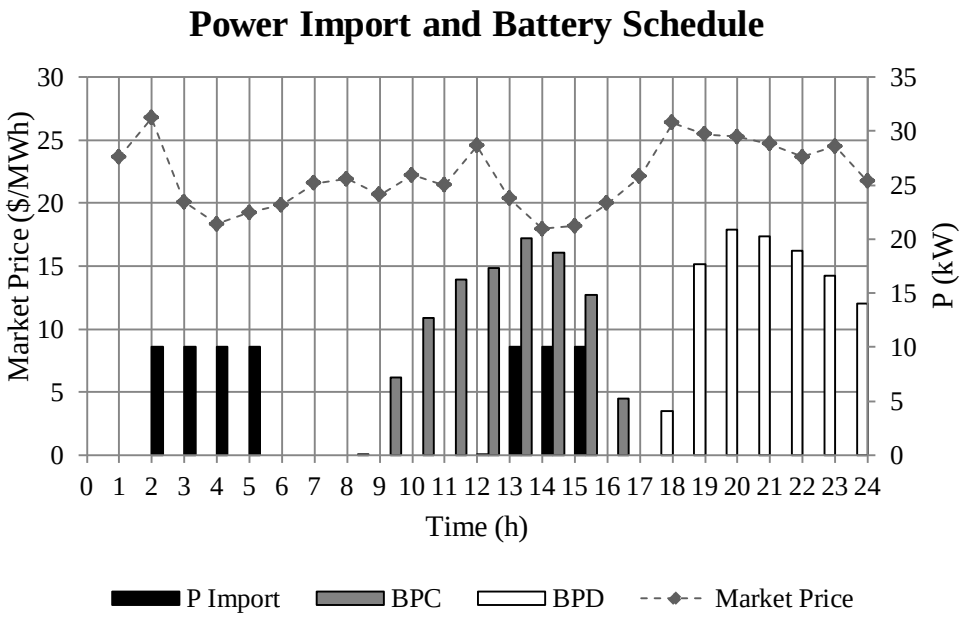

Figure 16 Power Import from Grid and Battery Schedule

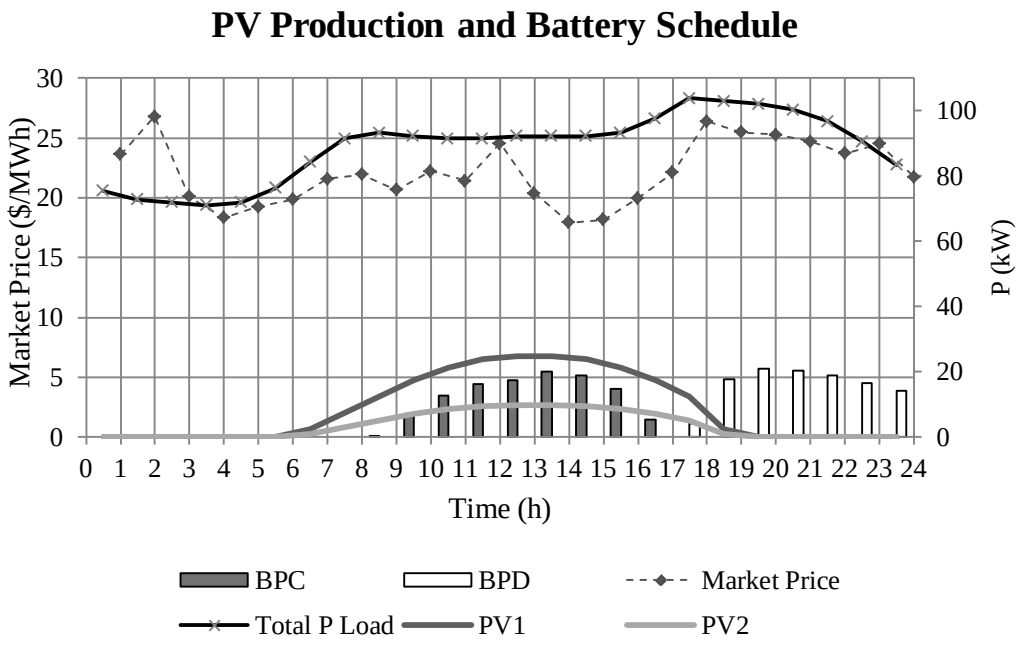

Figure 17 PV Array Power Production and Battery Schedule

The energy stored in the battery is discharged during t = 18 – 24 h, which are the peak load hours. The stored PV and imported energy is used to supply nearby loads and avoid looses if faraway AC generation were to supply these loads. Since the battery is not required to hold any energy at the end of 24 hours, it is economically beneficial to discharge all the battery energy so the net battery energy is 0. The total cost for supplying the load is $154.43 and the power loss is 157.7 kW.

The converter unknowns are shown in Table 3. Each converter has three unknowns as stated at the end of Chapter 3. The converter at AC bus 12 operates as a rectifier and the converter at AC bus 13 operates as an inverter as evidenced by the converter power factor angle representing the phase difference between the AC terminal bus fundamental voltage and current.

Table 3: Converter Unknowns

Time	**Transformer Tap AC Bus 12 Rectifier a**	**DC Current AC Bus 12 Rectifier I_{dc} (pu)**	**Converter Power Factor Angle AC Bus 12 Rectifier ϕ (radians)**	**Transformer Tap AC Bus 13 Inverter a**	**DC Current AC Bus 13 Inverter I_{dc} (pu)**	**Converter Power Factor Angle AC Bus 13 Rectifier ϕ (radians)**
1	0.745399	0.083402	0.275547	0.731705	0.076923	2.866974
2	0.745213	0.083174	0.275511	0.731552	0.076923	2.866974
3	0.745128	0.083097	0.275498	0.731467	0.076923	2.866974
4	0.745068	0.083021	0.275486	0.731419	0.076923	2.866974
5	0.745128	0.083097	0.275498	0.731467	0.076923	2.866974
6	0.745435	0.083479	0.275559	0.731718	0.076923	2.866974
7	0.745794	0.082876	0.275463	0.732172	0.078986	2.866639
8	0.745876	0.080909	0.275147	0.732533	0.083109	2.865971

9	0.745604	0.078511	0.274762	0.732608	0.087191	2.865312
10	0.74555	0.078492	0.274759	0.732556	0.087099	2.865327
11	0.745503	0.078515	0.274763	0.732503	0.086939	2.865353
12	0.745503	0.078515	0.274763	0.732503	0.086939	2.865353
13	0.74555	0.078492	0.274759	0.732556	0.087099	2.865327
14	0.745684	0.079514	0.274923	0.732532	0.085463	2.865591
15	0.745688	0.079538	0.274927	0.732532	0.085425	2.865597
16	0.745724	0.07944	0.274912	0.732583	0.085704	2.865552
17	0.745808	0.07823	0.274717	0.732851	0.08825	2.865141
18	0.746095	0.077915	0.274666	0.733184	0.089608	2.864923
19	0.746048	0.077952	0.274672	0.733132	0.089427	2.864952
20	0.746003	0.077994	0.274679	0.733078	0.089239	2.864982
21	0.745932	0.078072	0.274692	0.732995	0.08887	2.865042
22	0.745757	0.078255	0.274721	0.732797	0.088089	2.865167
23	0.745461	0.07859	0.274775	0.732456	0.086698	2.865392
24	0.745135	0.078912	0.274827	0.73208	0.085206	2.865632

5.4 Reserve

The battery is required to store energy to support the load for up to 1, 2, 3 or 4 hours ahead. The Reserve table in Appendix A lists the required reserve at each hour. The voltage solution is included in Appendix D. Since the reserve cases show similar results, only the results for the case of 4 hours ahead reserve is presented below.

5.4.1 Results (4 hr Reserve)

The generator schedule is shown in Figure 18. The large amount of generation in the 1st hour from generator 3 is required to charge the battery so that the load for 4 hours ahead can be served. The battery schedule in Figure 19 shows that the battery charging in the first hour overshadows the charging at any later hour. Since the initial energy in the battery is assumed to

be 0, the battery must hold enough energy at the end of the 1st hour to support the load for 4 hours ahead.

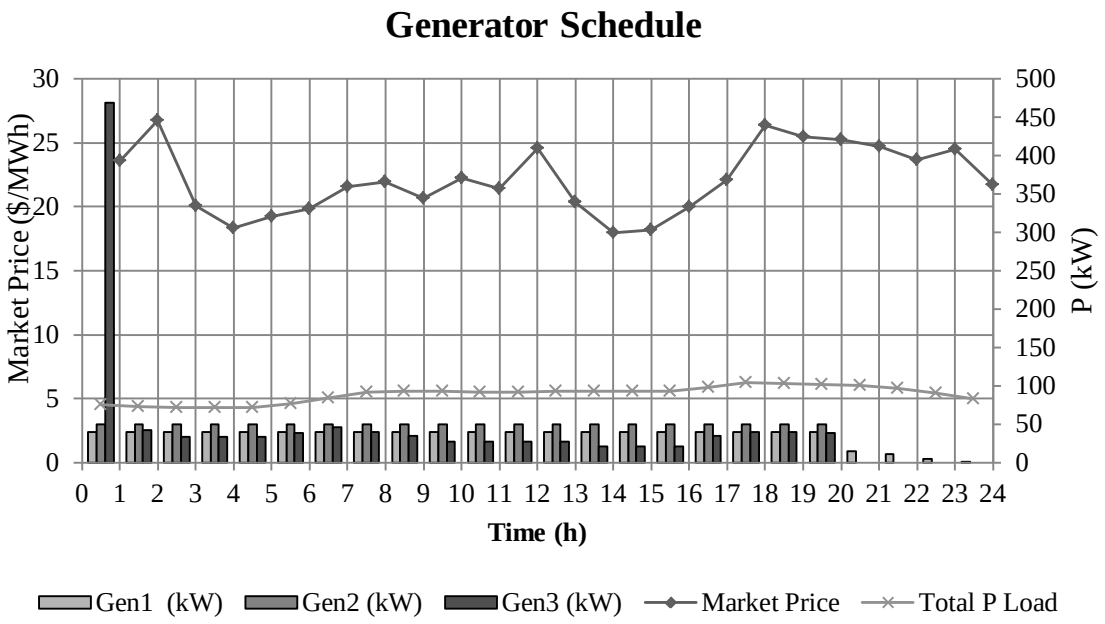

Figure 18 Generator Schedule

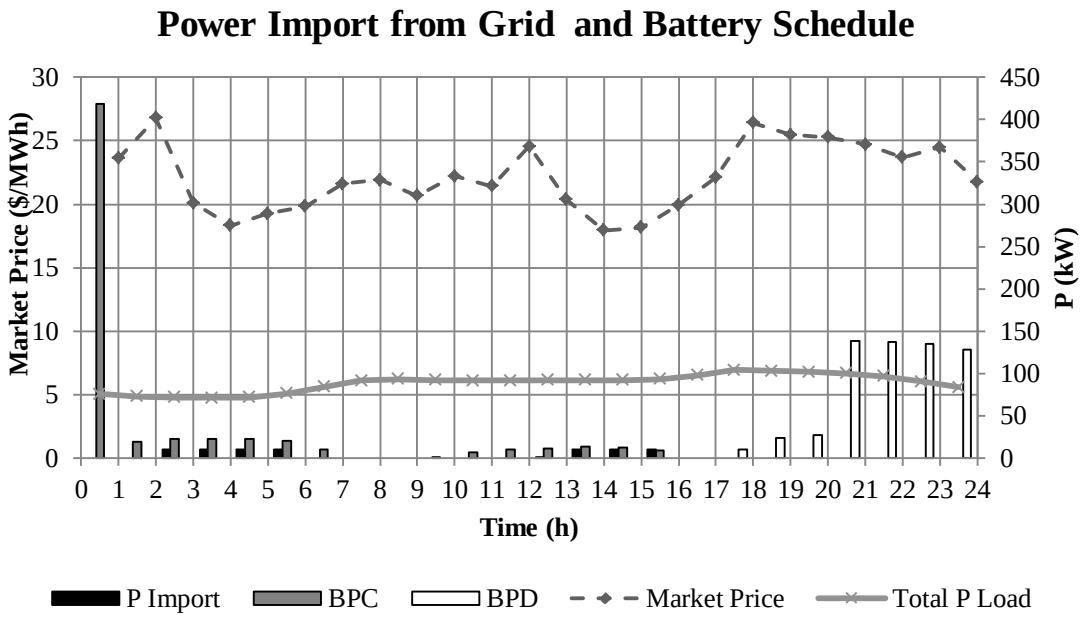

Figure 19 Power Import from Grid and Battery Schedule

The total cost of meeting power demand and the system power losses are shown in Figure 20. It can be seen that as more reserve is required, the cost increases slightly. This is due to the increase in losses also shown on the same figure. As more reserve energy is required, a large amount of energy has to be generated, mainly by generator 3, in the 1st hour to make sure reserve requirements for the next few hours are met and transferred to the battery which is located in the DC portion of the Microgrid.

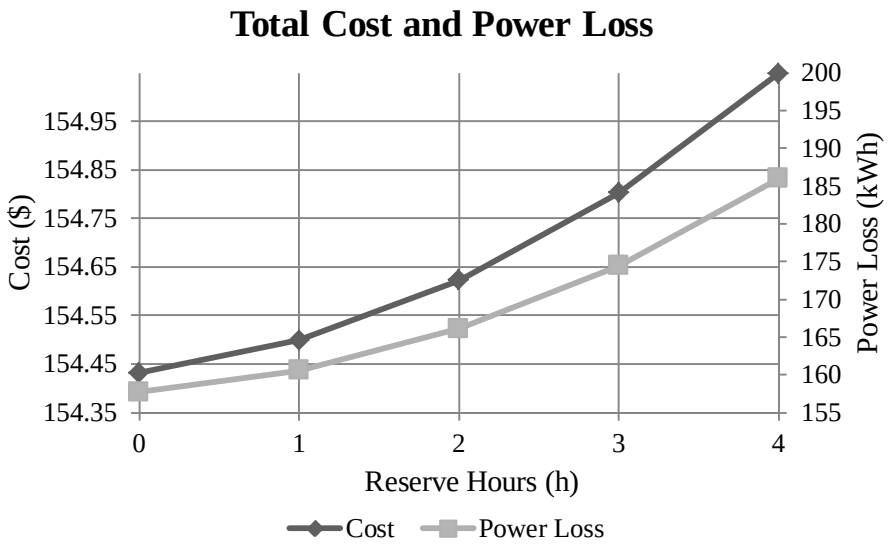

Figure 20 Total Cost and Power Loss

5.5 Energy in the Battery for Different Reserve Requirements

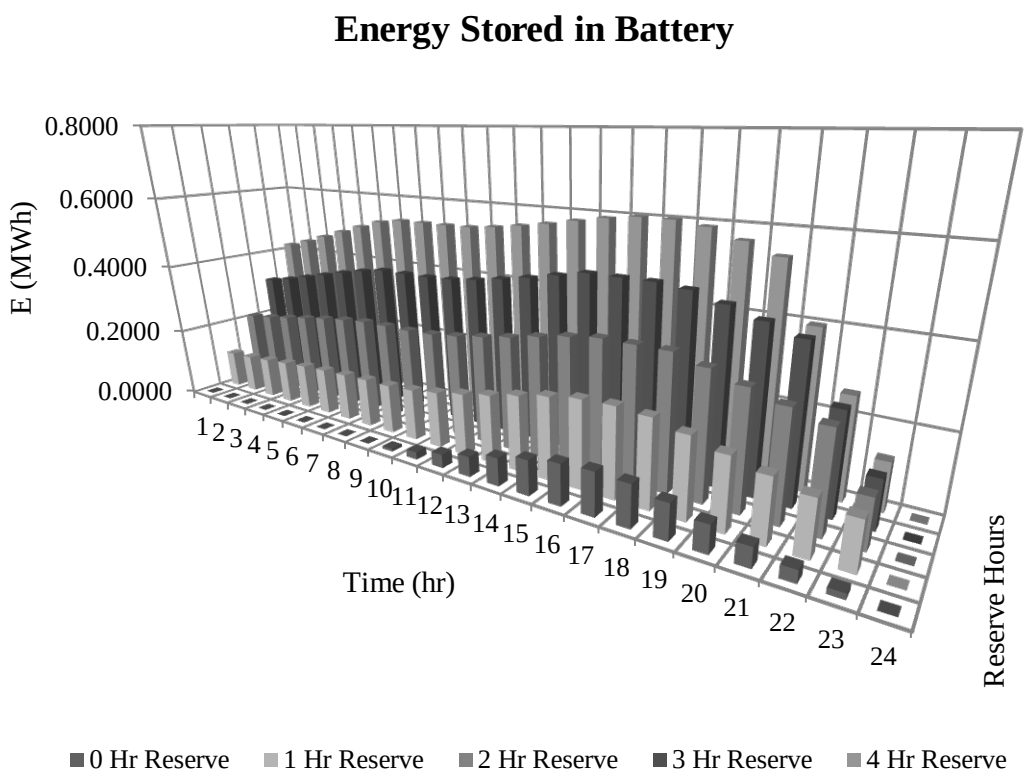

Figure 21 Energy in Battery for Reserve Requirements ranging from 0 to 4 hrs

The energy stored in the battery for different reserve requirements is shown in Figure 21. For the no reserve case, the battery charges from t = 10 to 17 h to store PV energy and energy imported from the grid, Figures 16 and 17, and then discharges to serve the load. The high power flow over the network during peak load hours is accompanied by high losses which are mitigated to some extent by the battery supplying nearby DC and AC loads during these hours. Less energy flowing into the DC network from the AC generation located far away leads to fewer losses and a lower cost. The 1 to 4 hour reserve cases in Figure 21 are similar so only the 4 hour reserve case will be examined to get vital information. For the 4 hour reserve case, the energy stored in the battery increases from t = 1 to 7 h and t = 10 to 16 h as the battery charges, Figure 19, to meet the reserve requirements and then the battery discharges to serve AC and DC loads during peak load hours after t = 17 h. The net battery energy at the end of 24 hours is 0 and so the generation cost should be approximately the same if the battery charge cycle cost is very low. The increase in cost as more reserve is required, shown in Figure 20, is because of the higher losses associated with charging the battery since the AC generation is located far away from where the battery is in the DC network. The increase in cost is very small because the power losses in both the AC and DC networks are very small.

5.6 Dual Objective – Minimize Cost and Maximize Reliability

The power import and the battery schedule from the grid are shown in Figure 22 where a 200 kWh battery is used. The battery is charged up to capacity in the first hour to ensure that the reliability index (RI) is kept high. Power is imported into the Microgrid whenever the import prices are lower (t = 3 to 6 h and t = 14 to 16 h) than the Microgrid generation cost. The battery charges between t = 10 to 16 h and this coincides with the time when power is imported and PV production is maximum. The battery discharges during peak load hours of t = 19 to 24 h. The total cost is $157.90.

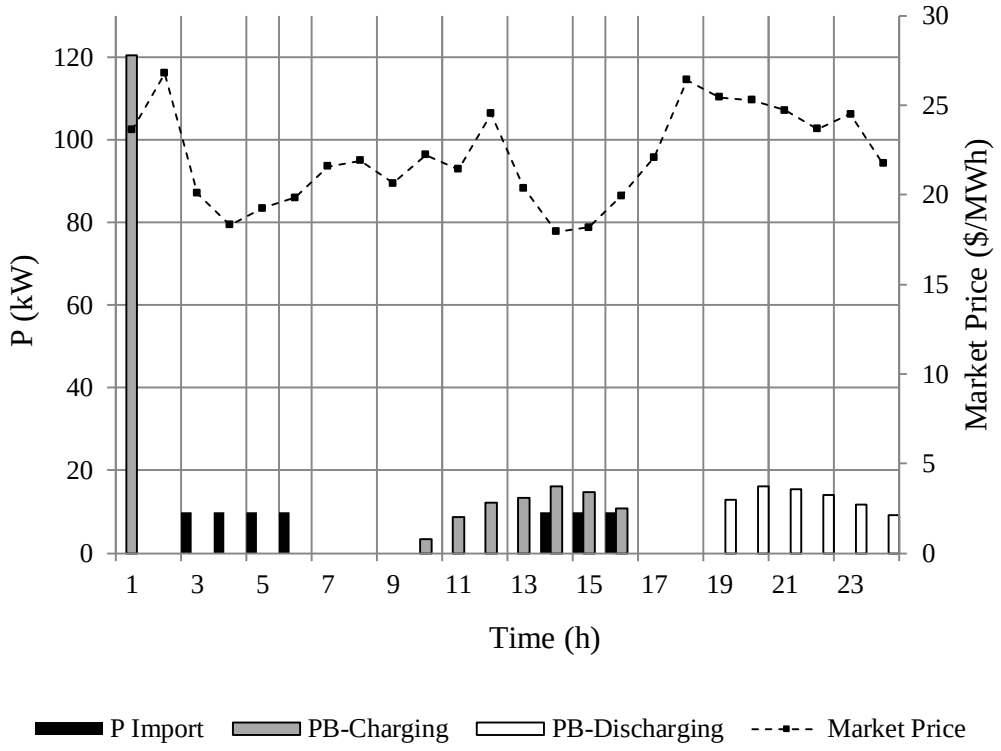

Figure 22 Power Import and Battery Schedule

The energy stored in the battery is given in Figure 23. The battery charges in the first hour and holds the charge to maintain a high RI. After the first hour, the battery starts charging at t = 10 until it reaches its capacity at t = 17 h and then discharges during peak load hours to serve the load. The battery discharge during peak load hours lowers costs slightly since the battery discharge will serve nearby loads leading to lower costs than if the far away AC generation were to serve these loads. The battery discharge lowers the energy stored in the battery and thus also lowers the reliability index; the reliability is sacrificed for lowering cost. The RI is 0.889 indicating that there are still hours when the battery is not able to meet the Microgrid load if needed. The conclusion to be drawn is that a larger battery may be needed to keep the RI above 1 at all times.

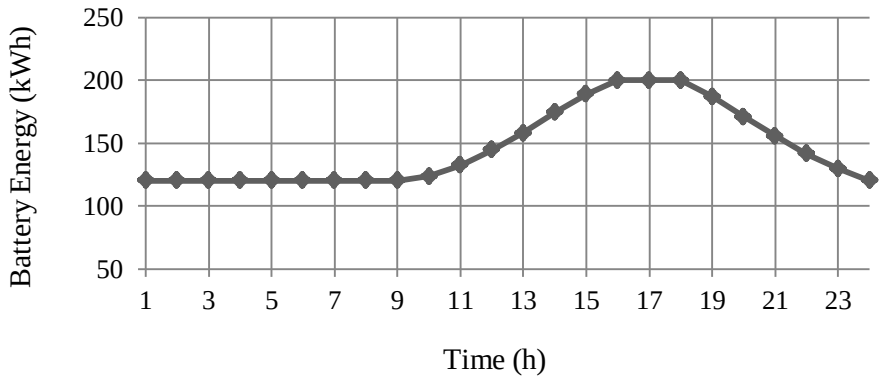

Figure 23 Energy Stored in Battery

The changes in the cost and reliability index due to the battery capacity are shown in Figure 24. A larger battery capacity improves the reliability by allowing the battery to hold more energy while still having enough energy to discharge to serve loads if necessary. The RI improves as the battery capacity is increased and the cost increases as well. The increase in cost is due to the energy stored in the battery that is never used and this is the cost of increased reliability. Considering the battery capacity used is 200 kWh and the RI is 0.889, the battery capacity needs to be changed to at least 250 kWh to have a RI above 1.

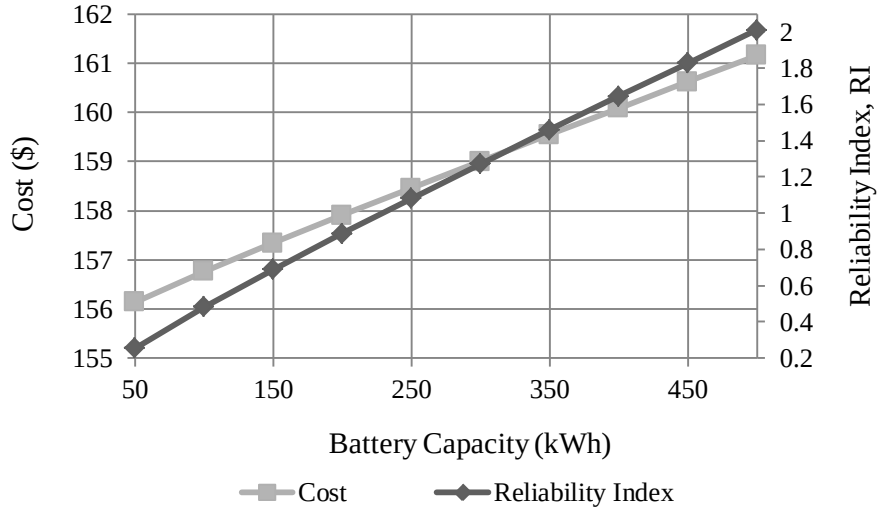

Figure 24 Cost and Reliability vs. Battery Capacity (kWh)

The RI can also be improved by increasing the minimum amount of energy held in the battery. The change in the RI and cost due to increasing the minimum amount of energy held in the battery is shown in Figure 25. In order to improve the RI to above 1, the battery needs to hold above 140 kWh at all times.

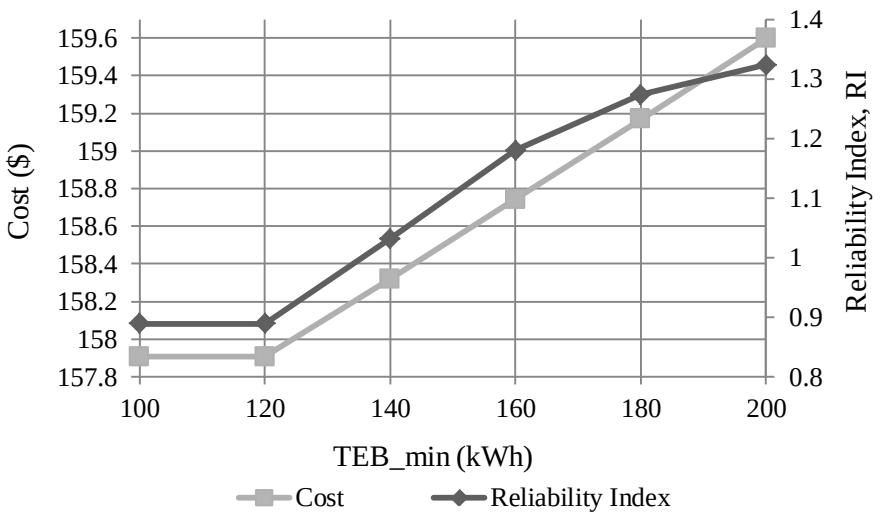

Figure 25 Cost and Reliability vs. Battery Capacity (kWh)

CHAPTER 6: CONCLUSIONS

This thesis considered the economic scheduling of an AC-DC Microgrid where AC generation, PV arrays, battery, grid power import and power converters are scheduled over 24 hours to satisfy load demands at minimum cost.

Although the Microgrid scheduling problem has been explored in publications such as [1]-[7], the case of hybrid AC and DC Microgrids has not been explored as much. The major contribution of this thesis was to examine the scheduling of a Microgrid which consists of separate AC and DC networks connected by power converters to exchange power. This allows DC based technologies such as batteries, PV arrays, fuel cells etc. to be separated from the AC system with the power converters being the power exchange interface. The harmonic suppression duties can be handled at a centralized location this way to enforce regulations.

The Microgrid scheduling results are presented in Chapter 5. The first objective examined was a purely economic objective in Sections 5.3, 5.4 and 5.5. It was found that when the battery is not required to hold any reserve, the battery charging and discharging coincides with PV array power production and grid power import as shown in Figures 16 and 17. The battery stores energy during low load times and discharges during peak load times. It may be necessary for the battery to hold reserve energy regardless of the economic repercussions. For example, a hospital may need a reliable backup energy source in case of a power outage or a business might find it beneficial to invest in energy storage rather than face the economic losses of being unable to do business. When the battery is required to hold reserve energy, the majority of the charging occurs during the first hour, Figure 19, to make sure that reserve energy is available for the upcoming hours. After the first hour, the battery charges in conjunction with power import from the grid and the PV arrays. Since there is no requirement for the battery to hold any reserve at the end of the scheduling period, the net battery energy at the end of 24 hours is 0. Hence, with or without battery reserve, the cost of satisfying the load demand should be approximately the same if the battery cycle cost is low. This is confirmed in Figure 20 where the cost increases slightly as more reserve is required. The increase in cost is due to losses. If reserve

is required then the battery will have to be charged in the first hour to make sure reserve requirements are met and as a result the high energy flow from the AC generator to the battery will result in higher losses and thus slightly higher costs. The energy profile of the battery for each hour and for each reserve case is shown in Figure 21.

The second objective considered is a dual objective given in Section 5.6. In this case, a solution is sought where cost is minimum and reliability is maximum. It was found that low costs restricted the reliability so that the battery could not hold energy up to its capacity but had to discharge to supply nearby loads to avoid costs associated with losses if the AC generation were to supply these loads. For the 200 kWh battery case examined, the reliability index indicated that a bigger battery might be required to maintain the index above 1 and still minimize costs. The two options investigated for increasing the RI above 1 were increasing the battery capacity and increasing the minimum amount of energy held in the 200 kWh battery.

As the battery capacity is increased, the following things are observed from Figure 24

- The reliability index, increases due to a large capacity battery being able to store more energy at any time and still being able to discharge to serve loads
- The increased reliability comes at the cost of energy stored in the battery that is never used and is required to maintain reliability
- At least a battery capable of storing 250 kWh is needed to ensure RI is above 1

As the minimum amount of energy held in the 200 kWh battery is increased, the following things are observed from Figure 25

- Both, the reliability index and cost, increase as the battery is required to hold more energy at all times
- For the 200 kWh battery, 140 kWh or above should be held in the battery to make sure RI is above 1

The most apparent extension of the Microgrid scheduling problem presented in this thesis is the formulation of a multi-objective problem where considerations other than economic are included into the scheduling process. Such a formulation could consider the scheduling of the

Microgrid in light of environmental, economic and technical restrictions since these concerns heavily influence the operation of a Microgrid.

APPENDICES

Appendix A: Altered IEEE 14-Bus System, Fig. 10

Base MVA: 1 MVA

The generator data for the AC generators at buses 1-3 and the power import generator at bus 8.

Generators Data

#	Bus Number	V (pu)	PMAX	Cost a_i ($/MWh^2)	Cost b_i ($/MWh)	Cost c_i ($/h)
1	1	1.06	40	0.02	20.1	1.4
2	2	1.045	50	0.02	20.15	1.3
3	3	1.01	650	0.02	20.25	1.25
4	8	1.04	10	NA	NA	NA

The transformer data for the AC network is given below.

Transformer Data

#	From Bus	To Bus	Resistance (pu)	Reactance (pu)	Off-Nominal Tap Ratio
1	5	6	0	0.25202	0.932
2	4	9	0	0.55618	0.969
3	4	7	0	0.20912	0.978

The transmission line data for the AC network is given below.

Transmission Line Data

#	From Number	To Number	Resistance (pu)	Reactance (pu)	Total Line Charging B (pu)	Tap
1	1	2	0.01938	0.05917	0.0528	0
2	1	5	0.05403	0.22304	0.0492	0
3	2	3	0.04699	0.19797	0.0438	0
4	2	4	0.05811	0.17632	0.0340	0
5	2	5	0.05695	0.17388	0.0346	0

6	3	4	0.06701	0.17103	0.0128	0
7	4	5	0.01335	0.04211	0	0
8	4	7	0	0.20912	0	0.978
9	4	9	0	0.55618	0	0.969
10	5	6	0	0.25202	0	0.932
11	6	11	0.09498	0.19890	0	0
12	6	12	0.12291	0.25581	0	0
13	6	13	0.06615	0.13027	0	0
14	7	8	0	0.17615	0	0
15	7	9	0	0.11001	0	0
16	9	10	0.03181	0.08450	0	0
18	9	14	0.12711	0.27038	0	0
19	10	11	0.08205	0.19207	0	0
20	12	13	0.22092	0.19988	0	0

The real power load data for the AC network is given below. The load data is given for each AC network bus at for 24 hours.

P Load Data for 24 Hours (1 MVA Base)

	Bus #	1	2	3	4	5	6	7	8
Time (h)									
1		0	0.01104	0.04806	0.0153	0	0	0.0012	0.0039
2		0	0.01068	0.04632	0.01476	0	0	0.0012	0.00372
3		0	0.01056	0.04578	0.01458	0	0	0.00114	0.00372
4		0	0.01044	0.04524	0.0144	0	0	0.00114	0.00366
5		0	0.01056	0.04578	0.01458	0	0	0.00114	0.00372
6		0	0.01122	0.0486	0.01548	0	0	0.00126	0.0039
7		0	0.01236	0.0537	0.0171	0	0	0.00138	0.00432
8		0	0.01344	0.0582	0.01854	0	0	0.0015	0.00468
9		0	0.01368	0.05934	0.0189	0	0	0.0015	0.0048
10		0	0.01356	0.0588	0.01872	0	0	0.0015	0.00474
11		0	0.01344	0.0582	0.01854	0	0	0.0015	0.00468
12		0	0.01344	0.0582	0.01854	0	0	0.0015	0.00468
13		0	0.01356	0.0588	0.01872	0	0	0.0015	0.00474

14		0	0.01356	0.0588	0.01872	0	0	0.0015	0.00474
15		0	0.01356	0.0588	0.01872	0	0	0.0015	0.00474
16		0	0.01368	0.05934	0.0189	0	0	0.0015	0.0048
17		0	0.01434	0.06216	0.0198	0	0	0.00156	0.00504
18		0	0.01524	0.06612	0.02106	0	0	0.00168	0.00534
19		0	0.01512	0.06558	0.02088	0	0	0.00168	0.00528
20		0	0.015	0.06498	0.0207	0	0	0.00168	0.00522
21		0	0.0147	0.06384	0.02034	0	0	0.00162	0.00516
22		0	0.01422	0.06162	0.01962	0	0	0.00156	0.00498
23		0	0.01326	0.05766	0.01836	0	0	0.00144	0.00468
24		0	0.01224	0.0531	0.01692	0	0	0.00138	0.00426

P Load Data for 24 Hours (1 MVA Base) (cont.)

	Bus #	9	10	11	12	13	14
Time (h)							
1		0	0.01164	0	0.00294	0.0057	0.00318
2		0	0.01122	0	0.00288	0.00552	0.00306
3		0	0.0111	0	0.00282	0.00546	0.003
4		0	0.01092	0	0.00276	0.0054	0.003
5		0	0.0111	0	0.00282	0.00546	0.003
6		0	0.01176	0	0.003	0.00576	0.00318
7		0	0.01302	0	0.0033	0.00636	0.00354
8		0	0.0141	0	0.0036	0.0069	0.00384
9		0	0.01434	0	0.00366	0.00708	0.0039
10		0	0.01422	0	0.0036	0.00696	0.00384
11		0	0.0141	0	0.0036	0.0069	0.00384
12		0	0.0141	0	0.0036	0.0069	0.00384
13		0	0.01422	0	0.0036	0.00696	0.00384
14		0	0.01422	0	0.0036	0.00696	0.00384
15		0	0.01422	0	0.0036	0.00696	0.00384
16		0	0.01434	0	0.00366	0.00708	0.0039
17		0	0.01506	0	0.00384	0.00738	0.00408
18		0	0.01602	0	0.00408	0.00786	0.00438
19		0	0.01584	0	0.00402	0.0078	0.00432

20		0	0.01572	0	0.00402	0.00774	0.00426
21		0	0.01548	0	0.00396	0.00762	0.0042
22		0	0.01494	0	0.00378	0.00732	0.00408
23		0	0.01398	0	0.00354	0.00684	0.00378
24		0	0.01284	0	0.0033	0.0063	0.00348

The reactive power load data for the AC network is given below. The load data is given for each AC network bus at for 24 hours.

Q Load Data for 24 Hours (1 MVA Base)

	Bus #	1	2	3	4	5	6	7	8
Time (h)									
1		0	0.00648	0.00972	0.0153	0	0	0.0006	0.00084
2		0	0.00624	0.00936	0.01476	0	0	0.0006	0.00078
3		0	0.00618	0.00924	0.01458	0	0	0.0006	0.00078
4		0	0.00612	0.00912	0.0144	0	0	0.0006	0.00078
5		0	0.00618	0.00924	0.01458	0	0	0.0006	0.00078
6		0	0.00654	0.00978	0.01548	0	0	0.0006	0.00084
7		0	0.00726	0.01086	0.0171	0	0	0.00066	0.0009
8		0	0.00786	0.01176	0.01854	0	0	0.00072	0.00096
9		0	0.00798	0.012	0.0189	0	0	0.00078	0.00102
10		0	0.00792	0.01188	0.01872	0	0	0.00072	0.00102
11		0	0.00786	0.01176	0.01854	0	0	0.00072	0.00096
12		0	0.00786	0.01176	0.01854	0	0	0.00072	0.00096
13		0	0.00792	0.01188	0.01872	0	0	0.00072	0.00102
14		0	0.00792	0.01188	0.01872	0	0	0.00072	0.00102
15		0	0.00792	0.01188	0.01872	0	0	0.00072	0.00102
16		0	0.00798	0.012	0.0189	0	0	0.00078	0.00102
17		0	0.0084	0.01254	0.0198	0	0	0.00078	0.00108
18		0	0.00894	0.01332	0.02106	0	0	0.00084	0.00114
19		0	0.00882	0.0132	0.02088	0	0	0.00084	0.00114
20		0	0.00876	0.01314	0.0207	0	0	0.00084	0.00108
21		0	0.00864	0.0129	0.02034	0	0	0.00084	0.00108
22		0	0.00828	0.01242	0.01962	0	0	0.00078	0.00102

23		0	0.0078	0.01164	0.01836	0	0	0.00072	0.00096
24		0	0.00714	0.01074	0.01692	0	0	0.00066	0.0009

Q Load Data for 24 Hours (1 MVA Base) (cont.)

	Bus #	9	10	11	12	13	14
Time (h)							
1		0	0.00558	0	0.00102	0.00384	0.00084
2		0	0.00534	0	0.00096	0.00372	0.00078
3		0	0.00528	0	0.00096	0.00366	0.00078
4		0	0.00522	0	0.00096	0.0036	0.00078
5		0	0.00528	0	0.00096	0.00366	0.00078
6		0	0.00564	0	0.00102	0.0039	0.00084
7		0	0.00624	0	0.00114	0.00426	0.0009
8		0	0.00672	0	0.00126	0.00462	0.00096
9		0	0.00684	0	0.00126	0.00474	0.00102
10		0	0.00678	0	0.00126	0.00468	0.00102
11		0	0.00672	0	0.00126	0.00462	0.00096
12		0	0.00672	0	0.00126	0.00462	0.00096
13		0	0.00678	0	0.00126	0.00468	0.00102
14		0	0.00678	0	0.00126	0.00468	0.00102
15		0	0.00678	0	0.00126	0.00468	0.00102
16		0	0.00684	0	0.00126	0.00474	0.00102
17		0	0.0072	0	0.00132	0.00498	0.00108
18		0	0.00768	0	0.00138	0.00528	0.00114
19		0	0.00756	0	0.00138	0.00522	0.00114
20		0	0.0075	0	0.00138	0.00516	0.00108
21		0	0.00738	0	0.00138	0.0051	0.00108
22		0	0.00714	0	0.00132	0.00492	0.00102
23		0	0.00666	0	0.0012	0.00462	0.00096
24		0	0.00612	0	0.00114	0.00426	0.0009

The price for importing energy into the Microgrid is shown in the table below. A real time pricing is assumed for importing energy into the Microgrid.

Market Price

Time (h)	Market Price ($/MWh)
1	23.62
2	26.78
3	20.09
4	18.32
5	19.26
6	19.85
7	21.59
8	21.92
9	20.66
10	22.23
11	21.43
12	24.54
13	20.37
14	17.94
15	18.18
16	19.96
17	22.1
18	26.4
19	25.45
20	25.28
21	24.72
22	23.69
23	24.5
24	21.75

The following table contains the reserve data for the Microgrid. When the battery is required to hold reserve energy then the table below gives values used. For example, 2 hr ahead reserve is the total load for the next 2 hours.

Reserve Data

Time (h)	Total P Load	1 Hr Ahead Reserve	2 hr Ahead Reserve	3 Hr Ahead Reserve	4 Hr Ahead Reserve
1	0.10976	0.10592	0.21056	0.31392	0.41856
2	0.10592	0.10464	0.208	0.31264	0.42368
3	0.10464	0.10336	0.208	0.31904	0.44172
4	0.10336	0.10464	0.21568	0.33836	0.4714
5	0.10464	0.11104	0.23372	0.36676	0.50236
6	0.11104	0.12268	0.25572	0.39132	0.52558
7	0.12268	0.13304	0.26864	0.4029	0.53594
8	0.13304	0.1356	0.26986	0.4029	0.53594
9	0.1356	0.13426	0.2673	0.40034	0.5346
10	0.13426	0.13304	0.26608	0.40034	0.5346
11	0.13304	0.13304	0.2673	0.40156	0.53582
12	0.13304	0.13426	0.26852	0.40278	0.53838
13	0.13426	0.13426	0.26852	0.40412	0.54618
14	0.13426	0.13426	0.26986	0.41192	0.56306
15	0.13426	0.1356	0.27766	0.4288	0.5786
16	0.1356	0.14206	0.2932	0.443	0.59152
17	0.14206	0.15114	0.30094	0.44946	0.59542
18	0.15114	0.1498	0.29832	0.44428	0.58512
19	0.1498	0.14852	0.29448	0.43532	0.56702
20	0.14852	0.14596	0.2868	0.4185	0.53984
21	0.14596	0.14084	0.27254	0.39388	0.39388
22	0.14084	0.1317	0.25304	0.25304	0.25304
23	0.1317	0.12134	0.12134	0.12134	0.12134
24	0.12134	0	0	0	0

Appendix B: DC Network, Fig. 11

The PV forecast data is given in the table below. The PV forecast for both arrays is assumed to be known.

PV Array Forecast Data

Time (h)	PV1 (kW)	PV2 (kW)
1	0	0
2	0	0
3	0	0
4	0	0
6	0	0
7	0	0
8	2.5	1
9	7.5	3
10	12.5	5
11	17.5	7
12	21.25	8.5
13	23.75	9.5
14	24.75	9.9
15	24.75	9.9
16	23.75	9.5
17	21.25	8.5
18	17.5	7
19	12.5	5
20	2.5	1
21	0	0
22	0	0
23	0	0
24	0	0

The DC load data for bus 1 of the DC network is given below. The DC load at all other buses is assumed to be 0.

DC Load Data

Time (h)	P (MW)
1	0.0068

2	0.00656
3	0.00648
4	0.0064
5	0.00648
6	0.00688
7	0.0076
8	0.00824
9	0.0084
10	0.00832
11	0.00824
12	0.00824
13	0.00832
14	0.00832
15	0.00832
16	0.0084
17	0.0088
18	0.00936
19	0.00928
20	0.0092
21	0.00904
22	0.00872
23	0.00816
24	0.00752

The DC network line resistance is given in the table below.

DC Network Line Resistance

#	From Branch	To Branch	Resistance (pu)
1	1	2	0.08
2	2	3	0.08
3	3	4	0.05
4	3	5	0.01
5	5	6	0.05
6	5	7	0.05
7	6	7	0.05

Appendix C: Converters

X_c = 0.05 pu for both converters

The control voltage and angle for the rectifier and inverter are given in the tables below.

Control Voltage Data

	Converter Voltage (pu)
AC Bus 12/DC Bus 2 Rectifier	1.05
AC Bus 13/DC Bus 4 Inverter	1.04

Control Angle Data

	Converter Angle (Degrees)
AC Bus 12/DC Bus 2 Rectifier Firing Angle	15
AC Bus 13/DC Bus 4 Inverter Extinction Advance Angle	15

Appendix D: Network Solution

This appendix contains the Voltage solution for network. The final values of the AC voltage and angles, and the DC voltage are given in the tables below.

No Reserve Case

The following solutions are for the case when no reserve is required to be held in the battery.

The table below gives the AC network nodal voltages for each hour.

AC Network Voltages (No Reserve Case)

	Bus	1	2	3	4	5	6	7
Time								
1		1.06	1.045	1.01	1.038807	1.040972	1.095677	1.068365
2		1.06	1.045	1.01	1.038867	1.041038	1.095889	1.068436
3		1.06	1.045	1.01	1.03904	1.041172	1.095989	1.068565
4		1.06	1.045	1.01	1.039059	1.041193	1.096055	1.068585
5		1.06	1.045	1.01	1.03904	1.041172	1.095989	1.068565
6		1.06	1.045	1.01	1.038943	1.041062	1.095644	1.068455
7		1.06	1.045	1.01	1.03866	1.040805	1.095071	1.068166
8		1.06	1.045	1.01	1.038592	1.04073	1.094654	1.068015
9		1.06	1.045	1.01	1.038634	1.040781	1.09463	1.067981
10		1.06	1.045	1.01	1.038654	1.040804	1.094698	1.068002
11		1.06	1.045	1.01	1.038671	1.040823	1.094767	1.068029
12		1.06	1.045	1.01	1.038671	1.040823	1.094767	1.068029
13		1.06	1.045	1.01	1.038654	1.040804	1.094698	1.068002
14		1.06	1.045	1.01	1.038774	1.040877	1.094683	1.068105
15		1.06	1.045	1.01	1.038773	1.040876	1.094682	1.068105
16		1.06	1.045	1.01	1.038757	1.040857	1.09462	1.068085
17		1.06	1.045	1.01	1.038558	1.040696	1.094316	1.067874
18		1.06	1.045	1.01	1.038451	1.040575	1.093884	1.06773
19		1.06	1.045	1.01	1.038469	1.040595	1.093952	1.067753
20		1.06	1.045	1.01	1.038486	1.040614	1.094021	1.067781
21		1.06	1.045	1.01	1.038513	1.040644	1.094131	1.067816
22		1.06	1.045	1.01	1.038576	1.040716	1.094387	1.067901
23		1.06	1.045	1.01	1.038685	1.040839	1.094828	1.068048
24		1.06	1.045	1.01	1.038808	1.040976	1.095318	1.068211

AC Network Voltages (No Reserve Case, cont.)

	Bus	8	9	10	11	12	13	14
Time								
1		1.04	1.089424	1.089908	1.09275	1.083966	1.093449	1.090849
2		1.04	1.089539	1.090065	1.092933	1.084225	1.093678	1.091029
3		1.04	1.089723	1.090246	1.093079	1.084346	1.093805	1.091194
4		1.04	1.089756	1.090293	1.093135	1.084429	1.093877	1.091244
5		1.04	1.089723	1.090246	1.093079	1.084346	1.093805	1.091194
6		1.04	1.089545	1.09	1.092785	1.083918	1.09343	1.090911
7		1.04	1.089081	1.089442	1.092214	1.083366	1.092855	1.090363
8		1.04	1.088799	1.089075	1.091819	1.08315	1.092523	1.090027
9		1.04	1.08871	1.088979	1.091754	1.083428	1.092615	1.09
10		1.04	1.088745	1.089026	1.091811	1.083506	1.092688	1.090056
11		1.04	1.088787	1.089081	1.091873	1.083575	1.092759	1.09012
12		1.04	1.088787	1.089081	1.091873	1.083575	1.092759	1.09012
13		1.04	1.088745	1.089026	1.091811	1.083506	1.092688	1.090056
14		1.04	1.088902	1.089161	1.091879	1.083361	1.092642	1.090128
15		1.04	1.088902	1.089161	1.091878	1.083357	1.092639	1.090127
16		1.04	1.088867	1.089114	1.091824	1.083299	1.092577	1.090076
17		1.04	1.088526	1.088731	1.091473	1.083117	1.092305	1.089741
18		1.04	1.08828	1.088398	1.091091	1.082686	1.091876	1.089386
19		1.04	1.088322	1.088456	1.091153	1.082756	1.091945	1.089443
20		1.04	1.088366	1.088511	1.091215	1.082823	1.092016	1.089512
21		1.04	1.088426	1.088594	1.091312	1.08293	1.092122	1.089596
22		1.04	1.08857	1.088786	1.091536	1.083193	1.092378	1.089806
23		1.04	1.08882	1.089125	1.091925	1.083639	1.092817	1.090167
24		1.04	1.089099	1.089504	1.092359	1.08413	1.093304	1.090566

The table below gives the AC network nodal angles for each hour.

AC Network Angles (No Reserve Case)

	Bus	1	2	3	4	5	6
Time							
1		0	0.003418	0.009466	0.000894	0.000518	-0.0064
2		0	0.003409	0.00927	0.000896	0.000535	-0.00621
3		0	0.00335	0.008334	0.001086	0.000719	-0.00559
4		0	0.003346	0.008265	0.001087	0.000726	-0.00552
5		0	0.00335	0.008334	0.001086	0.000719	-0.00559
6		0	0.003365	0.00867	0.001086	0.000689	-0.0059
7		0	0.003424	0.009823	0.000928	0.000534	-0.00653
8		0	0.003399	0.009723	0.000998	0.000643	-0.00601
9		0	0.003356	0.009212	0.001069	0.000788	-0.0051
10		0	0.003353	0.009152	0.001068	0.000792	-0.00505
11		0	0.003353	0.009119	0.001064	0.000789	-0.00504
12		0	0.003353	0.009119	0.001064	0.000789	-0.00504
13		0	0.003353	0.009152	0.001068	0.000792	-0.00505

14		0	0.003317	0.008543	0.00123	0.000905	-0.00491
15		0	0.003318	0.008549	0.001229	0.000904	-0.00492
16		0	0.003318	0.008579	0.001233	0.000907	-0.00493
17		0	0.003359	0.009386	0.001086	0.000798	-0.00516
18		0	0.003364	0.009652	0.001107	0.000805	-0.00528
19		0	0.003363	0.009606	0.001105	0.000806	-0.00525
20		0	0.003362	0.009572	0.001102	0.000803	-0.00524
21		0	0.003361	0.009496	0.001094	0.000801	-0.00521
22		0	0.003358	0.009348	0.001083	0.000797	-0.00514
23		0	0.003353	0.009081	0.001059	0.000786	-0.00503
24		0	0.003346	0.008774	0.001037	0.000779	-0.00488

AC Network Angles (No Reserve Case, cont.)

	Bus	7	8	9	10	11	12
Time							
1		-0.00123	-0.00123	-0.00196	-0.00323	-0.00472	-0.01192
2		-0.00112	-0.00112	-0.00181	-0.00305	-0.00454	-0.01169
3		0.00028	0.001865	-0.00073	-0.00205	-0.00372	-0.01102
4		0.000321	0.001906	-0.00067	-0.00198	-0.00365	-0.01094
5		0.00028	0.001865	-0.00073	-0.00205	-0.00372	-0.01102
6		0.000111	0.001697	-0.00097	-0.00233	-0.00402	-0.0114
7		-0.0014	-0.0014	-0.00218	-0.00351	-0.00493	-0.01197
8		-0.0013	-0.0013	-0.00203	-0.00335	-0.00459	-0.01114
9		-0.00099	-0.00099	-0.00159	-0.00283	-0.00389	-0.00985
10		-0.00095	-0.00095	-0.00154	-0.00278	-0.00383	-0.00979
11		-0.00094	-0.00094	-0.00152	-0.00275	-0.00381	-0.00978
12		-0.00094	-0.00094	-0.00152	-0.00275	-0.00381	-0.00978
13		-0.00095	-0.00095	-0.00154	-0.00278	-0.00383	-0.00979
14		0.000266	0.001852	-0.00073	-0.00208	-0.00341	-0.00978
15		0.000263	0.001848	-0.00073	-0.00209	-0.00342	-0.00979
16		0.000246	0.001832	-0.00075	-0.00211	-0.00344	-0.00979
17		-0.00107	-0.00107	-0.0017	-0.00297	-0.00399	-0.00987
18		-0.0012	-0.0012	-0.00187	-0.00318	-0.00415	-0.00994
19		-0.00117	-0.00117	-0.00183	-0.00314	-0.00412	-0.00991
20		-0.00115	-0.00115	-0.00181	-0.00311	-0.0041	-0.00991
21		-0.00112	-0.00112	-0.00177	-0.00306	-0.00406	-0.00989
22		-0.00105	-0.00105	-0.00167	-0.00294	-0.00396	-0.00984
23		-0.00093	-0.00093	-0.00151	-0.00274	-0.0038	-0.00979
24		-0.00077	-0.00077	-0.00129	-0.00248	-0.0036	-0.00969

AC Network Angles (No Reserve Case, cont.)

	Bus	13	14
Time			
1		-0.00259	-0.00257
2		-0.00239	-0.00239
3		-0.00169	-0.00147
4		-0.00162	-0.0014
5		-0.00169	-0.00147
6		-0.00204	-0.00177
7		-0.00259	-0.00274
8		-0.00172	-0.00231
9		-0.00044	-0.00151
10		-0.00039	-0.00145
11		-0.00039	-0.00144
12		-0.00039	-0.00144
13		-0.00039	-0.00145
14		-0.00034	-0.00097
15		-0.00035	-0.00098
16		-0.00034	-0.001
17		-0.00043	-0.00159
18		-0.00046	-0.00173
19		-0.00044	-0.0017
20		-0.00044	-0.00168
21		-0.00044	-0.00165
22		-0.00042	-0.00157
23		-0.0004	-0.00143
24		-0.00035	-0.00125

The table below gives the DC voltage at each bus of the DC network.

DC Network Voltages (No Reserve Case)

	Bus	1	2	3	4	5	6	7
Time								
1		1.049482	1.05	1.043846	1.04	1.043846	1.043846	1.043846
2		1.0495	1.05	1.043846	1.04	1.043846	1.043846	1.043846
3		1.049506	1.05	1.043846	1.04	1.043846	1.043846	1.043846
4		1.049512	1.05	1.043846	1.04	1.043846	1.043846	1.043846
5		1.049506	1.05	1.043846	1.04	1.043846	1.043846	1.043846
6		1.049476	1.05	1.043846	1.04	1.043846	1.043846	1.043846
7		1.049421	1.05	1.043949	1.04	1.043983	1.044079	1.044055
8		1.049372	1.05	1.044155	1.04	1.044256	1.044543	1.044471
9		1.04936	1.05	1.04436	1.04	1.044527	1.045005	1.044886
10		1.049366	1.05	1.044355	1.04	1.044589	1.045259	1.045092
11		1.049372	1.05	1.044347	1.04	1.044632	1.045445	1.045241
12		1.049372	1.05	1.044347	1.04	1.044665	1.045574	1.045346
13		1.049366	1.05	1.044355	1.04	1.044686	1.045633	1.045397

14		1.049366	1.05	1.044273	1.04	1.044605	1.045551	1.045315
15		1.049366	1.05	1.044271	1.04	1.044589	1.045498	1.045271
16		1.04936	1.05	1.044285	1.04	1.04457	1.045383	1.04518
17		1.049329	1.05	1.044412	1.04	1.044647	1.045317	1.045149
18		1.049286	1.05	1.04448	1.04	1.044648	1.045126	1.045007
19		1.049292	1.05	1.044471	1.04	1.044505	1.044601	1.044577
20		1.049299	1.05	1.044462	1.04	1.044462	1.044462	1.044462
21		1.049311	1.05	1.044443	1.04	1.044443	1.044443	1.044443
22		1.049335	1.05	1.044404	1.04	1.044404	1.044404	1.044404
23		1.049378	1.05	1.044335	1.04	1.044335	1.044335	1.044335
24		1.049427	1.05	1.04426	1.04	1.04426	1.04426	1.04426

4 Hr Reserve Case

The network solution for the 4 Hr Reserve case is given below.

The table below gives the AC network nodal voltages for each hour.

AC Network Voltages (4 Hr Reserve Case)

	Bus	1	2	3	4	5	6	7
Time								
1		1.06	1.045	1.01	1.028815	1.029187	1.065196	1.060709
2		1.06	1.045	1.01	1.038627	1.040757	1.095526	1.068385
3		1.06	1.045	1.01	1.038761	1.040846	1.095567	1.068505
4		1.06	1.045	1.01	1.038776	1.040863	1.095627	1.068524
5		1.06	1.045	1.01	1.038761	1.040846	1.095567	1.068505
6		1.06	1.045	1.01	1.038685	1.04076	1.095252	1.068399
7		1.06	1.045	1.01	1.038531	1.040654	1.094879	1.068139
8		1.06	1.045	1.01	1.038592	1.04073	1.094654	1.068015
9		1.06	1.045	1.01	1.038635	1.040782	1.094631	1.067981
10		1.06	1.045	1.01	1.038727	1.040889	1.094801	1.068015
11		1.06	1.045	1.01	1.038743	1.040907	1.094869	1.068042
12		1.06	1.045	1.01	1.038744	1.040908	1.094869	1.068042
13		1.06	1.045	1.01	1.038726	1.040889	1.0948	1.068015
14		1.06	1.045	1.01	1.038847	1.040962	1.094786	1.068118
15		1.06	1.045	1.01	1.038847	1.040962	1.094786	1.068118
16		1.06	1.045	1.01	1.03883	1.040942	1.094723	1.068098
17		1.06	1.045	1.01	1.038622	1.04077	1.094405	1.067885
18		1.06	1.045	1.01	1.038523	1.04066	1.093986	1.067742
19		1.06	1.045	1.01	1.038541	1.040679	1.094052	1.067766
20		1.06	1.045	1.01	1.038562	1.040702	1.094126	1.067794
21		1.06	1.045	1.01	1.039658	1.042031	1.095422	1.067823
22		1.06	1.045	1.01	1.039712	1.042094	1.09567	1.067906
23		1.06	1.045	1.01	1.039805	1.042203	1.096097	1.068047
24		1.06	1.045	1.01	1.039882	1.04229	1.096552	1.068209

AC Network Voltages (4 Hr Reserve Case, cont.)

	Bus	8	9	10	11	12	13	14
Time								
1		1.04	1.078549	1.075826	1.070858	1.027082	1.047292	1.064494
2		1.04	1.089559	1.090031	1.092751	1.082934	1.092945	1.090732
3		1.04	1.089745	1.090206	1.092866	1.082845	1.092953	1.090848
4		1.04	1.089779	1.090252	1.092919	1.082906	1.093012	1.090892
5		1.04	1.089745	1.090206	1.092866	1.082845	1.092953	1.090848

6		1.04	1.089565	1.089962	1.092587	1.082526	1.09264	1.090588
7		1.04	1.089094	1.089426	1.092119	1.082674	1.092464	1.090205
8		1.04	1.088799	1.089075	1.091819	1.08315	1.092523	1.090027
9		1.04	1.08871	1.088979	1.091754	1.083432	1.092617	1.090001
10		1.04	1.088732	1.08903	1.091859	1.083899	1.092905	1.090139
11		1.04	1.088775	1.089084	1.09192	1.083965	1.092974	1.090202
12		1.04	1.088775	1.089084	1.09192	1.083966	1.092975	1.090203
13		1.04	1.088732	1.08903	1.091858	1.083896	1.092904	1.090139
14		1.04	1.08889	1.089164	1.091927	1.083754	1.092859	1.090213
15		1.04	1.08889	1.089164	1.091927	1.083754	1.092859	1.090213
16		1.04	1.088855	1.089117	1.091872	1.083691	1.092794	1.09016
17		1.04	1.088516	1.088734	1.091514	1.083457	1.092492	1.089813
18		1.04	1.088268	1.088401	1.091138	1.083076	1.092091	1.089469
19		1.04	1.088309	1.088459	1.0912	1.083143	1.092158	1.089525
20		1.04	1.088352	1.088514	1.091264	1.083229	1.09224	1.089598
21		1.04	1.087829	1.088241	1.091682	1.089746	1.095562	1.090655
22		1.04	1.087971	1.088431	1.091901	1.089996	1.095811	1.090861
23		1.04	1.088218	1.088766	1.092282	1.090423	1.096238	1.091217
24		1.04	1.088521	1.089162	1.092711	1.090709	1.096629	1.091592

The table below gives the AC network nodal angles for each hour.

AC Network Angles (4 Hr Reserve Case)

	Bus	1	2	3	4	5	6
Time							
1		0	0.006442	0.049925	-0.00245	-0.00774	-0.07034
2		0	0.003547	0.011057	0.0007	0.000104	-0.00907
3		0	0.003509	0.010408	0.000858	0.000218	-0.00891
4		0	0.003508	0.01037	0.000856	0.000217	-0.00889
5		0	0.003509	0.010408	0.000858	0.000218	-0.00891
6		0	0.003513	0.010593	0.000875	0.000224	-0.00899
7		0	0.003499	0.010787	0.000822	0.000301	-0.00807
8		0	0.003399	0.009723	0.000998	0.000643	-0.00601
9		0	0.003355	0.009206	0.001069	0.000789	-0.00509
10		0	0.00331	0.008589	0.001131	0.000928	-0.00415
11		0	0.00331	0.008561	0.001126	0.000925	-0.00414
12		0	0.00331	0.008559	0.001127	0.000925	-0.00414
13		0	0.00331	0.008593	0.00113	0.000928	-0.00415
14		0	0.003274	0.007982	0.001292	0.001041	-0.00401
15		0	0.003274	0.007982	0.001292	0.001041	-0.00401
16		0	0.003275	0.00802	0.001295	0.001043	-0.00403
17		0	0.003321	0.008898	0.00114	0.000916	-0.00438
18		0	0.003321	0.009092	0.001169	0.000941	-0.00438
19		0	0.00332	0.009051	0.001167	0.000941	-0.00436
20		0	0.003317	0.008989	0.001166	0.000945	-0.0043

21		0	0.00337	0.007939	0.005555	0.005911	0.015058
22		0	0.003529	0.008364	0.005794	0.006109	0.015329
23		0	0.003817	0.009124	0.006223	0.006465	0.015808
24		0	0.004018	0.009789	0.006445	0.006601	0.015641

AC Network Angles (4 Hr Reserve Case, cont.)

	Bus	7	8	9	10	11	12
Time							
1		-0.02539	-0.02539	-0.03678	-0.04324	-0.05646	-0.10204
2		-0.00219	-0.00219	-0.00332	-0.00481	-0.00683	-0.01571
3		-0.00096	0.000627	-0.00248	-0.00408	-0.00639	-0.01568
4		-0.00094	0.000649	-0.00245	-0.00405	-0.00636	-0.01567
5		-0.00096	0.000627	-0.00248	-0.00408	-0.00639	-0.01568
6		-0.00104	0.000549	-0.00259	-0.00422	-0.0065	-0.01573
7		-0.00197	-0.00197	-0.003	-0.00445	-0.00617	-0.01414
8		-0.0013	-0.0013	-0.00203	-0.00335	-0.00459	-0.01114
9		-0.00098	-0.00098	-0.00158	-0.00283	-0.00388	-0.00984
10		-0.00062	-0.00062	-0.00106	-0.00223	-0.00311	-0.00852
11		-0.0006	-0.0006	-0.00105	-0.00221	-0.00309	-0.00852
12		-0.0006	-0.0006	-0.00105	-0.00221	-0.00309	-0.00852
13		-0.00062	-0.00062	-0.00107	-0.00223	-0.00311	-0.00853
14		0.000601	0.002187	-0.00025	-0.00153	-0.00269	-0.00852
15		0.000601	0.002187	-0.00025	-0.00153	-0.00269	-0.00852
16		0.000581	0.002166	-0.00028	-0.00157	-0.00271	-0.00853
17		-0.00078	-0.00078	-0.00128	-0.00249	-0.00336	-0.00877
18		-0.00086	-0.00086	-0.0014	-0.00263	-0.00343	-0.00868
19		-0.00084	-0.00084	-0.00136	-0.00259	-0.0034	-0.00866
20		-0.0008	-0.0008	-0.00132	-0.00254	-0.00334	-0.0086
21		0.00847	0.00847	0.010458	0.010587	0.012838	0.017465
22		0.00878	0.00878	0.010787	0.010933	0.013149	0.017706
23		0.009333	0.009333	0.011374	0.011549	0.013698	0.018122
24		0.009559	0.009559	0.011563	0.011731	0.013711	0.017682

AC Network Angles (4 Hr Reserve Case, cont.)

	Bus	13	14
Time			
1		-0.08803	-0.05921
2		-0.00632	-0.00496
3		-0.00627	-0.00445
4		-0.00626	-0.00444
5		-0.00627	-0.00445
6		-0.00628	-0.00454
7		-0.00471	-0.00413

8		-0.00172	-0.00231
9		-0.00043	-0.0015
10		0.000855	-0.00064
11		0.000845	-0.00064
12		0.00085	-0.00064
13		0.000847	-0.00064
14		0.000902	-0.00016
15		0.000902	-0.00016
16		0.000894	-0.00019
17		0.000651	-0.00088
18		0.000778	-0.00093
19		0.000787	-0.00089
20		0.000847	-0.00084
21		0.026501	0.017027
22		0.026717	0.017319
23		0.027098	0.017852
24		0.026624	0.017787

The table below gives the DC voltage at each bus of the DC network.

DC Network Voltages (4 Hr Reserve Case)

	Bus	1	2	3	4	5	6	7
Time								
1		1.049482	1.05	1.031359	1.04	1.031359	1.031359	1.031359
2		1.0495	1.05	1.04328	1.04	1.04328	1.04328	1.04328
3		1.049506	1.05	1.043189	1.04	1.043189	1.043189	1.043189
4		1.049512	1.05	1.043179	1.04	1.043179	1.043179	1.043179
5		1.049506	1.05	1.043189	1.04	1.043189	1.043189	1.043189
6		1.049476	1.05	1.043237	1.04	1.043237	1.043237	1.043237
7		1.049421	1.05	1.043644	1.04	1.043677	1.043773	1.043749
8		1.049372	1.05	1.044155	1.04	1.044256	1.044543	1.044471
9		1.04936	1.05	1.044361	1.04	1.044529	1.045007	1.044888
10		1.049366	1.05	1.044534	1.04	1.044768	1.045438	1.04527
11		1.049372	1.05	1.044524	1.04	1.044809	1.045622	1.045418
12		1.049372	1.05	1.044525	1.04	1.044843	1.045751	1.045524
13		1.049366	1.05	1.044532	1.04	1.044864	1.04581	1.045574
14		1.049366	1.05	1.044451	1.04	1.044783	1.045729	1.045493
15		1.049366	1.05	1.044451	1.04	1.044769	1.045678	1.045451
16		1.04936	1.05	1.044463	1.04	1.044747	1.04556	1.045357
17		1.049329	1.05	1.044567	1.04	1.044802	1.045471	1.045304
18		1.049286	1.05	1.044658	1.04	1.044825	1.045304	1.045184
19		1.049292	1.05	1.044648	1.04	1.044681	1.044777	1.044753
20		1.049299	1.05	1.044647	1.04	1.044647	1.044647	1.044647
21		1.049311	1.05	1.047923	1.04	1.047923	1.047923	1.047923
22		1.049335	1.05	1.047881	1.04	1.047881	1.047881	1.047881

23		1.049378	1.05	1.047808	1.04	1.047808	1.047808	1.047808
24		1.049427	1.05	1.047624	1.04	1.047624	1.047624	1.047624

REFERENCES

1. H. Z. Liang and H. B. Gooi, “Unit commitment in microgrids by improved genetic algorithm,” in *IPEC Conference Proceedings*, 2010, pp. 842-847.
2. N. D. Hatziargyriou, A. Dimeas, A. G. Tsikalakis, J. A. Lopes, G. Kariniotakis, and J. Oyarzabal, “Management of microgrids in market environment,” in *International Conference on Future Power Systems*, 2005, p. 7.
3. A. G. Tsikalakis and N. D. Hatziargyriou, “Centralized control for optimizing microgrids operation,” *IEEE Transactions on Energy Conversion*, vol. 23, no. 1, pp. 241-248, 2008.
4. M. Y. Nguyen, Y. T. Yoon, and N. H. Choi, “Dynamic programming formulation of micro-grid operation with heat and electricity constraints,” in *Transmission & Distribution Conference & Exposition: Asia and Pacific*, 2009, pp. 1-4.
5. C. A. Hernandez-Aramburo, T. C. Green, and N. Mugniot, “Fuel consumption minimization of a microgrid,” *IEEE Transactions on Industry Applications*, vol. 41, no. 3, pp. 673-681, 2005.
6. T. Logenthiran and D. Srinivasan, “Short term generation scheduling of a microgrid,” in *TENCON - IEEE Region 10 Conference*, 2009, pp. 1-6.
7. C. Yuen, A. Oudalov, and A. Timbus, “The provision of frequency control reserves from multiple microgrids,” *IEEE Transactions on Industrial Electronics*, vol. 58, no. 1, pp. 173-183, 2011.
8. R. Lasseter et al., “The CERTS microgrid concept - integration of distributed energy,” 2002.
9. E. Sanchez, J. Santiago, and J. Oyarzabal, “Novel concepts for microgrids: dc networks,” 2007.
10. Arrillaga, J., & Smith, B. (1998). AC-DC Power System Analysis. London: The Institution of Electrical Engineers.
11. Kundur, P. (1994). Power System Stability and Control. McGraw-Hill Professional.

12. Kothari, D. & Dhillon, J. (2008). Power Systems Optimization. McGraw-Hill.
13. M. W. Mustafa and A. F. A. Kadir, “A modified approach for load flow analysis of integrated ac-dc power systems,” in *TENCON Proceedings*, 2000, pp. 108-113.
14. A. Panosyan and B. R. Oswald, “Modified newton-raphson load flow analysis for integrated ac/dc power systems,” in 39th International Universities Power Engineering Conference, 2004, pp. 1223-1227.
15. O. Osaloni and G. Radman, “Integrated ac/dc systems power flow solution using newton-raphson and broyden approaches,” in *Proceedings of the Thirty-Seventh Southeastern Symposium on System Theory*, 2005, pp. 225-229.
16. Y. Mobarak, “Modified load flow analysis for integrated ac/dc power systems,” in *12th International Middle-East Power System Conference*, 2008, pp. 402-405.
17. Glover, J. D., Sarma, M. S., & Overbye, T. J. (2007). Power System Analysis and Design. Nelson Education Ltd.
18. A. Dukpa, I. Duggal, B. Venkatesh, and L. Chang, “Optimal participation and risk mitigation of wind generators in an electricity market,” *IET Renewable Power Generation*, vol. 4, no. 2, pp. 165-175, 2010.